Journal of Nonlinear Science (2022) 32:88
https://doi.org/10.1007/s00332-022-09840-7

Journal of Nonlinear Science

The Spin–Spin Problem in Celestial Mechanics

Alessandra Celletti[1] · **Joan Gimeno**[2] · **Mauricio Misquero**[3]

Received: 13 October 2021 / Accepted: 14 August 2022

Abstract

We study the dynamics of two homogeneous rigid ellipsoids subject to their mutual gravitational influence. We assume that the spin axis of each ellipsoid coincides with its shortest physical axis and is perpendicular to the orbital plane. Due to such assumptions, the problem is planar and depends on particular parameters of the ellipsoids, most notably, the equatorial oblateness and the flattening with respect to the shortest physical axes. We consider two models for such configuration: while in the full model, there is a coupling between the orbital and rotational motions, in the Keplerian model, the centers of mass of the bodies are constrained to move on coplanar Keplerian ellipses. The Keplerian case, in the approximation that includes the coupling between the spins of the two ellipsoids, is what we call spin–spin problem, that is a generalization of the classical spin–orbit problem. In this paper we continue the investigations of Misquero (Nonlinearity 34:2191–2219, 2021) on the spin–spin problem by comparing

Communicated by Amadeu Delshams.

A.C. acknowledges GNFM-INdAM and the MIUR Excellence Department Project awarded to the Department of Mathematics, University of Rome Tor Vergata, CUP E83C18000100006, EU-ITN Stardust-R and MIUR-PRIN 20178CJA2B "New Frontiers of Celestial Mechanics: theory and Applications." J.G. has been supported by the Spanish grants PGC2021-125535NB-I00, PGC2021-122954NB-I00, and with funds from NextGenerationEU within the Spanish national Recovery, Transformation and Resilience plan.

✉ Joan Gimeno
jgimeno@ub.edu

Alessandra Celletti
celletti@mat.uniroma2.it

Mauricio Misquero
mmisquero@ugr.es

[1] Department of Mathematics, University of Rome Tor Vergata, Via della Ricerca Scientifica 1, 00133 Rome, Italy

[2] Departament de Matemàtiques i Informàtica, Universitat de Barcelona, Gran Via de les Corts Catalanes, 585, 08007 Barcelona, Spain

[3] Departamento de Didáctica de la Matemática, Universidad de Granada, Campus Universitario de Cartuja 18071, Granada, Spain

Published online: 19 September 2022

it with the spin–orbit problem and also with the full model. Beside detailing the models associated to the spin–orbit and spin–spin problems, we introduce the notions of standard and balanced resonances, which lead us to investigate the existence of periodic and quasi-periodic solutions. We also give a qualitative description of the phase space and provide results on the linear stability of solutions for the spin–orbit and spin–spin problems. We conclude by providing a comparison between the full and the Keplerian models with particular reference to the interaction between the rotational and orbital motions.

Keywords Spin–spin model · Spin–orbit model · Two-body problem · Resonances · Periodic orbits · Quasi-periodic solutions

Mathematics Subject Classification 37N05 · 70F15 · 70E50

1 Introduction

The dynamics of two rigid bodies orbiting under their mutual gravitational attraction is a classical problem of Celestial Mechanics known as the *Full Two-Body problem*. In this context, Kinoshita investigated the problem by using Hori–Deprit perturbation theory (Kinoshita 1972), assuming that one of the bodies is spherical and the other body is triaxial. Later, the problem of two extended rigid bodies was studied in Maciejewski (1995) as a Hamiltonian system with respect to a non-canonical structure, which is used to characterize the relative equilibria. A seminal work was performed in Boué (2017) to which we refer for an alternative description of the model of the full two rigid body problem using spherical harmonics and Wigner D-matrices. In Scheeres (2009), the problem is restricted to a planar configuration with the potential expanded to order $1/r^3$, where r is the relative distance between the two rigid bodies; under this condition, Scheeres (2009) describes the relative equilibria and their stability properties.

In this paper, we investigate different simplified models of rotational dynamics of celestial bodies, subject to the mutual gravitational attraction. The spin–spin problem was introduced in Misquero (2021) as a planar version of the Full Two-Body problem for ellipsoids (compare with Batygin and Morbidelli 2015; Boué and Laskar 2009), by using the expansion of the potential up to order $1/r^5$, which results in the coupling of the spins of both bodies. An equivalent model was studied in Nadoushan and Assadian (2016b) (see also Hou and Xin 2017).

Indeed, we consider a hierarchy of models with different complexity. In particular, we start by considering two homogeneous rigid ellipsoidal bodies subject to the following assumptions:

Assumption 1 The spin axis of each ellipsoid is perpendicular to the orbital plane.

Assumption 2 The spin axis of each ellipsoid is aligned with the shortest physical axis of the satellite.

Assumptions 1 and 2 imply that the motion takes place on a plane. Following Misquero (2021), we introduce a Hamiltonian function that includes both the orbital

and rotational motions. Using the conservation of the angular momentum, the system is described by a Hamiltonian with 3 degrees of freedom that depends on several parameters of each ellipsoid, among which there are the equatorial oblateness and the flattening with respect to the shortest physical axis. Such parameters are typically small for natural bodies of the solar system. We refer to this model as the *full* problem, since it includes the coupling between the orbital and rotational motions.

The potential of the problem can be written as $V = V_0 + \sum_{l=1}^{\infty} V_{2l}$, where V_0 denotes the Keplerian potential and the terms V_{2l} are proportional to $1/r^{2l+1}$, where r is the instantaneous distance of the two centers of mass. If we consider the expansion up to order $l = 2$, say $V = V_0 + V_2 + V_4$, we obtain that the model includes the coupling of the spins of the two ellipsoids. The term V_2 is such that the rotation angles of the two satellites appear within separate trigonometric terms, while the term V_4 contains also combinations of the rotation angles. When the two spins interact, we refer to the problem as the *full spin–spin* model. We refer to the *full spin–orbit model*, when we limit the potential to $V = V_0 + V_2$.

Next, we introduce another assumption, namely:

Assumption 3 The orbital motion of the ellipsoids coincides with that of two point masses, so that both centers of mass move on coplanar Keplerian orbits with eccentricity $e \in [0, 1)$ and with a common focus at the barycenter of the system.

Assumption 3 implies that the orbit is not affected by the rotational motion. To the *full* spin–spin and spin–orbit problems, it corresponds the *Keplerian* spin–spin and spin–orbit models, described by a Hamiltonian function with an explicit periodic time dependence. When one of the bodies is spherical, its spin is uniform and the dynamics of the spin–spin model becomes very similar to that of the spin–orbit model, but including the terms in V_4 (see, e.g., Beletskii 1966; Celletti 1990; Goldreich and Peale 1966). The decoupled equation of motion for the study of the rotational dynamics under Assumption 3 has been widely studied in the literature within different contexts, e.g. the rotation of Mercury (Colombo and Shapiro 1966), the obliquity of the planets (Laskar and Robutel 1993), capture probabilities (Goldreich and Peale 1966), or the chaotic rotation of Hyperion (Wisdom et al. 1984). It must be clear that such assumption poses a big constraint on the orbital motion, which can be accepted under special conditions, for example when the celestial bodies have a nearly spherical shape.

Note that we are considering rigid bodies only, which means that dissipative effects due to tidal torques are not considered. We refer to Celletti and Chierchia (2008), Celletti and Chierchia (2009), Misquero and Ortega (2020), Misquero (2021) and Goldreich and Peale (1966) for a description of the dissipative spin–orbit and spin–spin problems.

The previously described models have some symmetries that are a direct consequence of the mirror symmetries of the ellipsoids. This fact leads us to introduce the following two types of resonances within the spin–orbit problem of a single ellipsoid:

(**R1**) We call *standard* $m : n$ spin–orbit resonance, for some integers m, n, when the spinning body makes m rotations during n orbital revolutions;
(**R2**) We call *balanced* $m : 2$ spin–orbit resonance, for some integers m, when the spinning body makes $m/2$ of a rotation during one orbital revolution.

We remark that a balanced spin–orbit resonance is also a standard resonance, but the converse is not always true. For example, a balanced $2k : 2$ resonance for $k \in \mathbb{Z}$ is equivalent to a $k : 1$ spin–orbit resonance, but there is not such an equivalence for order $(2k + 1) : 2$. Both definitions (**R1**) and (**R2**) extend to the spin–spin problem of type $(m_1 : n_1, m_2 : n_2)$ for integers m_1, m_2, n_1, n_2, when the first ellipsoid is in a $m_1 : n_1$ spin–orbit resonance and the second ellipsoid in a $m_2 : n_2$ spin–orbit resonance.

We also stress that spin–orbit resonances find many applications in the solar system; in fact, the Moon is an example of a $1 : 1$ spin–orbit resonance,[1] since it makes a rotation in the same period it takes to make an orbit around the Earth. This is also called a *synchronous* spin–orbit resonance, which is common to many satellites of other planets, including Mars, Jupiter, Saturn, Uranus, Neptune. Among the planets, Mercury is locked in a $3 : 2$ spin–orbit resonance around the Sun. On the other hand, the Pluto-Charon system is locked in the double synchronous spin–spin resonance $(1 : 1, 1 : 1)$.

In this work, we study the behavior of the solutions of the spin–orbit and spin–spin problems as the parameters and the initial conditions are varied. In particular, we investigate the boundary conditions that lead to the existence of symmetric periodic orbits. Such results (see Propositions 5 and 10) use some symmetry properties of the equations of motion. We remark that these symmetries are lost if we include dissipation; however, such periodic solutions might be continued to the dissipative setting as shown in Misquero and Ortega (2020) and Misquero (2021). Beside the study of the periodic orbits, we provide the conditions for the existence of quasi-periodic solutions of the Keplerian version of the spin–spin model.

We also give a qualitative study of the spin–orbit problem as well as the spin–spin problem with spherical and non-spherical companion. Within such investigation, we discover some new features, like the measure synchronization (see, e.g., Hampton and Zanette 1999) for the spin–spin problem with identical bodies. Our study leads to analyze the multiplicity of solutions and the linear stability of the periodic orbits (compare with Celletti and Chierchia 2000). In general, we find that there is not a unique solution associated to a particular resonance; however, for some values of the parameters such a uniqueness exists. Finally, we provide some results on the full and Keplerian models, as well as on the interaction between the spin and the orbital motion, motivated by the role that the coupling between the rotational and orbital motions takes in planetary sciences, especially in connection to asteroid binary systems (see, e.g., Kinoshita 1972; Maciejewski 1995; Scheeres 2002, 2009; Bellerose and Scheeres 2008).

This work is organized as follows. In Sect. 2 we present the spin–orbit and spin–spin models. The definition of resonances and the existence of periodic and quasi-periodic orbits are given in Sect. 3. A qualitative description of the phase space is given in Sect. 4. The linear stability of symmetric periodic orbits is investigated in Sect. 5. Finally, a comparison between the full and Keplerian models is presented in Sect. 6.

[1] A $2 : 2$ balanced spin–orbit resonance is equivalent to a $1 : 1$ standard spin–orbit resonance.

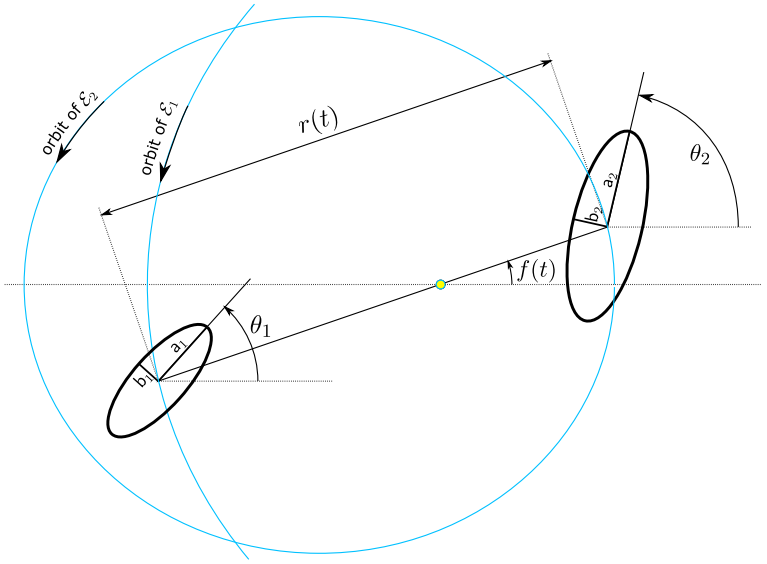

Fig. 1 The planar spin–spin problem considering Assumptions 1 to 3

2 The Models for the Spin–Orbit and Spin–Spin Coupling

The aim of this section is to present the so-called *spin–orbit* and *spin–spin* models, that we are going to introduce as follows. The assumptions and the notations are given in Sect. 2.1; different models, subject to some or all the assumptions listed in Sect. 2.1, are presented in Sects. 2.2 and 2.3.

2.1 General Assumptions

Consider two homogeneous rigid ellipsoids, say $\mathcal{E}_1$ and $\mathcal{E}_2$, with masses M_1 and M_2, respectively. Let $\mathcal{A}_j < \mathcal{B}_j < \mathcal{C}_j$, $j = 1, 2$, be their principal moments of inertia with corresponding principal semi-axes $\mathsf{a}_j > \mathsf{b}_j > \mathsf{c}_j$. We refer to the *Full Two-Body Problem* (hereafter F2BP) as the problem of two rigid bodies interacting gravitationally (see, e.g., Scheeres 2002, 2009). When the bodies have ellipsoidal shape, we speak of the *ellipsoidal F2BP*, where we make the Assumptions 1, 2, 3 of Sect. 1:

Assumptions 1 and 2 guarantee that the problem we deal with is a planar problem. Additionally, Assumption 3 restricts the problem so that we obtain a model with two degrees of freedom and a periodic time dependence. This assumption is equivalent to say that the spin motion will not influence the orbital motion. Besides, note that we are neglecting the gravitational contribution of other bodies, we are not considering any dissipative effect that might arise, for example, from the non-rigidity of the ellipsoidal bodies and we do not take into account the obliquity, namely the inclination of the spin-axes with respect to the orbital plane (Fig. 1).

We are going to work with units adapted to the system. If we call τ the orbital period of the Keplerian orbit, then we will use units such that

$$M_1 + M_2 = 1, \quad \mathcal{C}_1 + \mathcal{C}_2 = 1, \quad \tau = 2\pi.$$

Recall Kepler's third law for the Two-Body Problem

$$G(M_1 + M_2)\left(\frac{\tau}{2\pi}\right)^2 = a^3,$$

where G is the gravitational constant, a is the semi-major axis associated to the motion of the reduced mass of the system, say $\mu = M_1 M_2$ in our units. In consequence, $G = a^3$ in our units.

Let us now define the parameters for each ellipsoid

$$d_j = \mathcal{B}_j - \mathcal{A}_j, \quad q_j = 2\mathcal{C}_j - \mathcal{B}_j - \mathcal{A}_j;$$

the quantity $d_j/\mathcal{C}_j$ measures the equatorial oblateness of each ellipsoid with respect to the plane formed by the directions of a_j and b_j, whereas $q_j/\mathcal{C}_j$ measures the flattening with respect to the direction corresponding to the c_j-axis.

Note that if $\mathcal{A}_j \leq \mathcal{B}_j \leq \mathcal{C}_j$, then, in our units there are some bounds for the parameters of the system given by

$$0 \leq d_j \leq \mathcal{C}_j \leq 1, \quad d_j \leq q_j \leq 2\mathcal{C}_j \leq 2, \quad M_j \mathsf{a}_j^2 = \frac{5}{2}(\mathcal{C}_j + d_j) \leq 5\mathcal{C}_j \leq 5. \quad (1)$$

The last relation in (1) comes from the fact that the moments of inertia of an ellipsoid hold the identities

$$\mathcal{A}_j = \frac{1}{5} M_j(\mathsf{b}_j^2 + \mathsf{c}_j^2), \quad \mathcal{B}_j = \frac{1}{5} M_j(\mathsf{a}_j^2 + \mathsf{c}_j^2), \quad \mathcal{C}_j = \frac{1}{5} M_j(\mathsf{a}_j^2 + \mathsf{b}_j^2).$$

2.2 The Full Models

First, let us derive the equations of the full models of spin–orbit and spin–spin coupling, for which only Assumptions 1 and 2 hold, namely we do not constrain the centers of mass of $\mathcal{E}_1$ and $\mathcal{E}_2$ to move on Keplerian ellipses.

The equations of motion are obtained by computing the Hamiltonian function through a Legendre transformation of the Lagrangian, say $L = T - V$, where T is the kinetic energy and V the potential energy of the system. We split T in two parts, associated respectively to the orbital and rotational motions, say $T = T_{\text{orb}} + T_{\text{rot}}$.

Let us identify the orbital plane with the complex plane $\mathbb{C}$, consider the center of mass of the system fixed in the origin and let the position of each ellipsoid be $\mathbf{r}_j \in \mathbb{C}$. Then, by definition of the barycenter we have

$$M_1 \mathbf{r}_1 + M_2 \mathbf{r}_2 = \mathbf{0}.$$

If we define the relative position vector $\mathbf{r} = \mathbf{r}_2 - \mathbf{r}_1$, since in our units $M_1 + M_2 = 1$, then we have

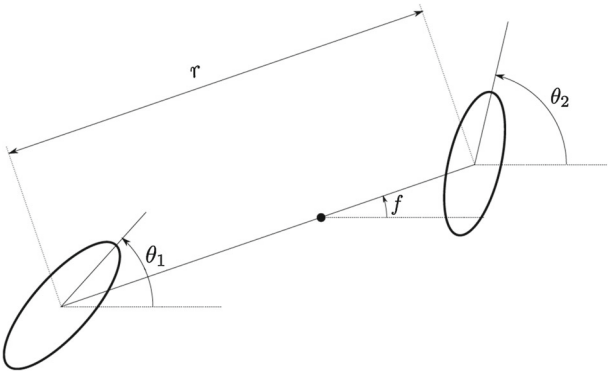

Fig. 2 Generalized coordinates of the full planar model

$$\mathbf{r}_1 = -M_2\mathbf{r}, \quad \mathbf{r}_2 = M_1\mathbf{r}. \tag{2}$$

We introduce the Lagrangian generalized coordinates $(r, f, \theta_1, \theta_2)$, illustrated in Fig. 2, in the following way. The distance $r > 0$ and the angle f define the relative position vector $\mathbf{r} = r\exp(if) \in \mathbb{C}$ with respect to an inertial reference frame with a fixed x-axis. The angles θ_1, θ_2 provide the orientation of the axes $\mathsf{a}_1, \mathsf{a}_2$ with respect to the x-axis. The variables r and f define the orbital motion of the system and θ_j the spin motion of the ellipsoid $\mathcal{E}_j$.

To write the kinetic energy, we notice that we can express $\mathbf{r}$ in components as $\mathbf{r} = (r\cos f, r\sin f)$, which gives $\dot{\mathbf{r}} = (\dot{r}\cos f - r\dot{f}\sin f, \dot{r}\sin f + r\dot{f}\cos f)$. Then, using (2), the total orbital and the rotational kinetic energies are given by

$$T_{\text{orb}} = \frac{1}{2}(M_1\dot{\mathbf{r}}_1^2 + M_2\dot{\mathbf{r}}_2^2) = \frac{\mu}{2}\dot{\mathbf{r}}^2 = \frac{\mu}{2}(\dot{r}^2 + r^2\dot{f}^2), \quad T_{\text{rot}} = \frac{1}{2}\mathcal{C}_1\dot{\theta}_1^2 + \frac{1}{2}\mathcal{C}_2\dot{\theta}_2^2,$$

where $\mu = M_1M_2$ in our units. The Lagrangian is given by

$$L(r, f, \theta_1, \theta_2, \dot{r}, \dot{f}, \dot{\theta}_1, \dot{\theta}_2) = T_{\text{orb}}(r, \dot{r}, \dot{f}) + T_{\text{rot}}(\dot{\theta}_1, \dot{\theta}_2) - V(r, f, \theta_1, \theta_2),$$

where, according to Misquero (2021) and Boué (2017), the full expansion of the potential energy of the system $V = V(r, f, \theta_1, \theta_2)$ takes the form

$$V(r, f, \theta_1, \theta_2) = -\frac{GM_1M_2}{r} \sum_{\substack{(l_1,m_1)\in\Upsilon \\ (l_2,m_2)\in\Upsilon}} \frac{\Lambda_{l_2,m_2}^{l_1,m_1}}{r^{2(l_1+l_2)}} \cos(2m_1(\theta_1 - f) + 2m_2(\theta_2 - f)), \tag{3}$$

where

$$\Upsilon = \{(l, m) \in \mathbb{Z}^2 : 0 \le |m| \le l\},$$

and the constants $\Lambda_{l_2,m_2}^{l_1,m_1}$ are defined in "Appendix A"; we refer to Misquero (2021) for full details.

Let us define the momenta as

$$p_r = \partial_{\dot{r}} L = \mu \dot{r}, \quad p_f = \partial_{\dot{f}} L = \mu r^2 \dot{f}, \quad p_j = \partial_{\dot{\theta}_j} L = \mathcal{C}_j \dot{\theta}_j;$$

then, the Hamiltonian of the system becomes

$$H(r, f, \theta_1, \theta_2, p_r, p_f, p_1, p_2) = \frac{p_r^2}{2\mu} + \frac{p_f^2}{2\mu r^2} + \frac{p_1^2}{2\mathcal{C}_1} + \frac{p_2^2}{2\mathcal{C}_2} + V(r, f, \theta_1, \theta_2). \tag{4}$$

Consequently, the equations of motion are

$$\dot{r} = \frac{p_r}{\mu}, \quad \dot{f} = \frac{p_f}{\mu r^2}, \quad \dot{p}_r = \frac{p_f^2}{\mu r^3} - \partial_r V, \quad \dot{p}_f = -\partial_f V \tag{5}$$

and

$$\dot{\theta}_j = \frac{p_j}{\mathcal{C}_j}, \quad \dot{p}_j = -\partial_{\theta_j} V. \tag{6}$$

We remark that with these variables, the problem splits in two parts: Eq. (5) describe the *orbital* motion, while Eq. (6) describe the *rotational* motion. The evolution of both parts is coupled through the potential V.

The potential V, expanded in (3), can be written in a perturbative way as

$$V(r, f, \theta_1, \theta_2) = V_0(r) + V_{\text{per}}(r, f, \theta_1, \theta_2), \quad V_0(r) = -\frac{GM_1M_2}{r}. \tag{7}$$

We remark that the term V_0 corresponds to the classical Keplerian form for the potential and the term V_{per} provides the coupling between the spin and the orbital motions. Moreover, we can expand V_{per} as $V_{\text{per}} = \sum_{l=1}^{\infty} V_{2l}$, where V_{2l} are suitable terms proportional to $1/r^{2l+1}$. A truncation of the expansion of V_{per} will result in an approximated dynamics of our system. The explicit expressions of the first two terms of such a expansion are given in Misquero (2021) and we report them here:

$$\begin{aligned}
V_2 &= -\frac{GM_2}{4r^3}\left(q_1 + 3d_1\cos(2\theta_1 - 2f)\right) - \frac{GM_1}{4r^3}\left(q_2 + 3d_2\cos(2\theta_2 - 2f)\right), \\
V_4 &= -\frac{3G}{4^3r^5}\left\{12q_1q_2 + \frac{15}{7}\left[\frac{M_2}{M_1}d_1^2 + 2\frac{M_2}{M_1}q_1^2 + \frac{M_1}{M_2}d_2^2 + 2\frac{M_1}{M_2}q_2^2\right]\right. \\
&\quad + d_1M_2\left\{\left[20\frac{q_2}{M_2} + \frac{100}{7}\frac{q_1}{M_1}\right]\cos(2\theta_1 - 2f) + 25\frac{d_1}{M_1}\cos(4\theta_1 - 4f)\right\} \\
&\quad + d_2M_1\left\{\left[20\frac{q_1}{M_1} + \frac{100}{7}\frac{q_2}{M_2}\right]\cos(2\theta_2 - 2f) + 25\frac{d_2}{M_2}\cos(4\theta_2 - 4f)\right\} \\
&\quad \left. + 6d_1d_2\cos(2\theta_1 - 2\theta_2) + 70d_1d_2\cos(2\theta_1 + 2\theta_2 - 4f)\right\}.
\end{aligned} \tag{8}$$

From now on, we will refer to (5) and (6) as the full models: *full spin–orbit model* if we take $V_{\text{per}} = V_2$, in which the angles θ_1, θ_2 appear in different trigonometric terms, and *full spin–spin model* if $V_{\text{per}} = V_2 + V_4$, which contains trigonometric terms with combinations of the rotation angles θ_1, θ_2. These names are motivated by the well-known spin–orbit model, Celletti (2010), and the spin–spin model from Misquero (2021). If we consider the models under Assumption 3 which gives a constraint on the orbit, we speak of *Keplerian spin–orbit model* and *Keplerian spin–spin model* (compare with Sect. 2.3).

2.2.1 Conservation of the Angular Momentum

Note that the Hamiltonian H in (4) is invariant under the transformation $(r, f, \theta_1, \theta_2) \mapsto (r, f+\delta f, \theta_1+\delta f, \theta_2+\delta f)$, where δf is an infinitesimal angular increase, because the angular arguments of $V(r, f, \theta_1, \theta_2)$ only depend on the differences $\theta_1 - f$ and $\theta_2 - f$. This symmetry is related, by Noether's theorem (Goldstein 1980), with a conserved quantity, say, the total angular momentum $p_f + p_1 + p_2$. This can be proved through the following change of variables

$$(r, f, \theta_1, \theta_2, p_r, p_f, p_1, p_2) \mapsto (r, f, \phi_1, \phi_2, p_r, P_f, p_1, p_2),$$

where

$$\phi_j = \phi_j(f, \theta_j) = \theta_j - f, \quad P_f = P_f(p_f, p_1, p_2) = p_f + p_1 + p_2. \tag{9}$$

The transformation of coordinates (9) is canonical, since

$$\mathrm{d}r \wedge \mathrm{d}p_r + \mathrm{d}f \wedge \mathrm{d}p_f + \sum_{j=1}^{2} \mathrm{d}\theta_j \wedge \mathrm{d}p_j = \mathrm{d}r \wedge \mathrm{d}p_r + \mathrm{d}f \wedge \mathrm{d}P_f + \sum_{j=1}^{2} \mathrm{d}\phi_j \wedge \mathrm{d}p_j.$$

Then, the Hamiltonian (4) in this new set of variables is given by

$$\mathcal{H}(r, f, \phi_1, \phi_2, p_r, P_f, p_1, p_2) = \frac{p_r^2}{2\mu} + \frac{(P_f - p_1 - p_2)^2}{2\mu r^2} + \frac{p_1^2}{2\mathcal{C}_1} + \frac{p_2^2}{2\mathcal{C}_2} + \mathcal{V}(r, \phi_1, \phi_2), \tag{10}$$

where $\mathcal{V}(r, \phi_1, \phi_2) = V(r, f, \phi_1 + f, \phi_2 + f)$. Now it is clear that f is an ignorable variable in (10) and that P_f is a constant of motion, corresponding to the total angular momentum of the system.

In summary, in the evolution of the system, there is a transfer of angular momentum between the spin part, given for each body by $p_j = \mathcal{C}_j \dot{\theta}_j$, and the orbital part, given by $p_f = \mu r^2 \dot{f}$.

2.3 The Keplerian Models

In this section, we introduce the Assumption 3 to the model of Sect. 2.2. From (5) and (6), it is straightforward to constrain the orbit to be Keplerian; only in the orbital part

we retain just the term V_0 of the potential $V = V_0 + V_{\text{per}}$ in (7), thus obtaining the following equations:

$$\dot{r} = \frac{p_r}{\mu}, \quad \dot{f} = \frac{p_f}{\mu r^2}, \quad \dot{p}_r = \frac{p_f^2}{\mu r^3} - \partial_r V_0, \quad \dot{p}_f = -\partial_f V_0 = 0, \tag{11}$$

and

$$\dot{\theta}_j = \frac{p_j}{\mathcal{C}_j}, \quad \dot{p}_j = -\partial_{\theta_j} V = -\partial_{\theta_j} V_{\text{per}}. \tag{12}$$

A convenient procedure to numerically integrate the equations of motion (12) is presented in "Appendix B".

2.3.1 Orbital Motion

Note that since $\partial_{\theta_j} V_0 = 0$, the system (11) is now decoupled from (12). Moreover, (11) is the Kepler problem, whose solutions depend on the eccentricity e and the semi-major axis a of the orbit. Here we assume for simplicity that the orbit is a 2π-periodic Keplerian ellipse of eccentricity $e \in [0, 1)$ with focus at the origin and with the periapsis on the positive x-axis.

Since the orbital period is 2π, then we can take the time t to coincide with the *mean anomaly*. We denote by u the *eccentric anomaly*, which, in our units, is related to the mean anomaly by Kepler's equation

$$t = u - e \sin u. \tag{13}$$

The orbital radius is related to u by

$$r = a(1 - e \cos u). \tag{14}$$

We can write the vector $\mathbf{r} \in \mathbb{C}$ in terms of the eccentric anomaly also as

$$r \exp(if) = a(\cos u - e + i\sqrt{1 - e^2} \sin u). \tag{15}$$

Note that for $t = 0$ we assumed, without loss of generality, that $f = u = 0$, and consequently, $f = u = \pi$ when $t = \pi$. From (15) we obtain the following useful relations between f and u

$$\cos f = \frac{\cos u - e}{1 - e \cos u}, \quad \sin f = \frac{\sqrt{1 - e^2} \sin u}{1 - e \cos u}. \tag{16}$$

With the previous definitions, the Keplerian orbit of eccentricity e and semi-major axis a is given by the functions

$$r = r(t; a, e), \quad f = f(t; e), \quad p_r = p_r(t; a, e), \quad p_f = p_f(a, e) = \mu a^2 \sqrt{1 - e^2}, \tag{17}$$

that correspond to the solution of Eq. (11) generated by the initial conditions

$$r(0) = a(1-e), \quad p_r(0) = 0, \quad f(0) = 0, \quad p_f(0) = \mu a^2\sqrt{1-e^2}. \tag{18}$$

2.3.2 Spin Motion

The spin motion is described by Eq. (12) with the Keplerian periodic input (17) given implicitly by Eqs. (13) to (15). This motion can be described by the non-autonomous Hamiltonian

$$H_K(t, \theta_1, \theta_2, p_1, p_2) = H(r(t; a, e), f(t; e), \theta_1, \theta_2, p_r(t; a, e), p_f(a, e), p_1, p_2), \tag{19}$$

where $H(r, f, \theta_1, \theta_2, p_r, p_f, p_1, p_2)$ is the Hamiltonian of the full model defined in (4). The Hamiltonian (19) is hence of the form

$$H_K(t, \theta_1, \theta_2, p_1, p_2) = \frac{p_1^2}{2\mathcal{C}_1} + \frac{p_2^2}{2\mathcal{C}_2} + W(t, \theta_1, \theta_2), \tag{20}$$

where the potential W is 2π-periodic in t and π-periodic in θ_1 and θ_2. The equations of motion (12) take the form

$$\dot{\theta}_j = \frac{p_j}{\mathcal{C}_j}, \quad \dot{p}_j = -\partial_{\theta_j} W(t, \theta_1, \theta_2). \tag{21}$$

Let us define the non-dimensional parameters of the model:

$$\lambda_j = 3\frac{\mu}{M_j}\frac{d_j}{\mathcal{C}_j}, \quad \sigma_j = \frac{1}{3}\frac{\mathcal{C}_j}{\mu a^2}, \quad \hat{q}_j = \frac{q_j}{M_j a^2}, \tag{22}$$

where λ_j represents the equatorial oblateness of $\mathcal{E}_j$; σ_j is the ratio between the moment of inertia of $\mathcal{E}_j$ and the orbital one; and $\hat{q}_j$ measures the flattening of $\mathcal{E}_j$ with respect to the size of the orbit. Note that the parameters in (22) are small for bodies that are close to spherical. Besides, not all the parameters defined previously are free, because we have the constraint $\mathcal{C}_1\sigma_2 = \mathcal{C}_2\sigma_1$.

If we take $V_{\text{per}} = V_2$, then the system (12) becomes

$$\ddot{\theta}_j + \frac{\lambda_j}{2}\left(\frac{a}{r(t; e)}\right)^3 \sin(2\theta_j - 2f(t; e)) = 0, \quad j = 1, 2, \tag{23}$$

that is a system of two uncoupled spin–orbit problems. Each of these problems depends just on two parameters: (e, λ_j). On the other hand, if $V_{\text{per}} = V_2 + V_4$, from (12) and (8) we obtain the following system for $j = 1, 2$,

$$0 = \ddot{\theta}_j + \frac{\lambda_j}{2}\left\{\left(\frac{a}{r(t; e)}\right)^3 \sin(2\theta_j - 2f(t; e))\right.$$

$$+\left(\frac{a}{r(t;e)}\right)^5\left[\frac{5}{4}\left(\hat{q}_{3-j}+\frac{5}{7}\hat{q}_j\right)\sin(2\theta_j-2f(t;e))\right.$$
$$+\frac{25}{8}\lambda_j\sigma_j\sin(4\theta_j-4f(t;e))+\lambda_{3-j}\sigma_{3-j}\left(\frac{3}{8}\sin(2\theta_j-2\theta_{3-j})\right.$$
$$\left.\left.+\frac{35}{8}\sin(2\theta_{3-j}+2\theta_j-4f(t;e))\right)\right]\Bigg\}, \tag{24}$$

that we call spin–spin problem. From the previous discussion, this model depends on seven independent parameters[2] $(e;\mathcal{C}_1,\lambda_1,\lambda_2,\sigma_1,\hat{q}_1,\hat{q}_2)$. Note that in (24), the coupling between the dynamics of θ_1 and θ_2 is given by σ_1 and σ_2. Moreover, if $\hat{q}_j=\sigma_j=0$, the spin–spin problem (24) is reduced to a pair of spin–orbit problems (23).

Let us now consider (24) in the case that $\mathcal{E}_2$ is a sphere, that is, $d_2=q_2=0$. Then, $\lambda_2=\sigma_2=\hat{q}_2=0$, which implies that $\mathcal{E}_2$ is in uniform rotation $\theta_2(t)=\dot{\theta}_2(0)t+\theta_2(0)$. The dynamics of θ_1 is uncoupled from θ_2 and is given by

$$0=\ddot{\theta}_1+\frac{\lambda_1}{2}\left\{\left(\frac{a}{r(t;e)}\right)^3\sin(2\theta_1-2f(t;e))\right.$$
$$\left.+\left(\frac{a}{r(t;e)}\right)^5\left[\frac{25\hat{q}_1}{28}\sin(2\theta_1-2f(t;e))+\frac{25\lambda_1\sigma_1}{8}\sin(4\theta_1-4f(t;e))\right]\right\}, \tag{25}$$

that is a spin–orbit problem up to order $1/r^5$. An equivalent system was studied previously in Nadoushan and Assadian (2016a). Here the parameters σ_1 and $\hat{q}_1$ perturb the framework of the spin–orbit problem (23).

2.3.3 Reversing Symmetries

The equations for the spin motion in the Keplerian models have some reversing symmetries, i.e., transformations in the phase space that keep invariant the equations of motion with a time reversal.

Definition 1 Consider the differential equation

$$\frac{\mathrm{d}\mathbf{x}}{\mathrm{d}t}=\mathbf{F}(\mathbf{x}),\quad \mathbf{x}\in\mathbb{R}^n, \tag{26}$$

and let $\mathbf{x}(t;\mathbf{x}_0)$ be the solution of (26) with initial condition $\mathbf{x}(0;\mathbf{x}_0)=\mathbf{x}_0$.

(1) A transformation $R:\mathbb{R}^n\to\mathbb{R}^n$ is called a reversing symmetry of (26) if

$$\frac{\mathrm{d}R(\mathbf{x})}{\mathrm{d}t}=-\mathbf{F}(R(\mathbf{x})).$$

[2] In Misquero (2021) there was an error because $\hat{q}_1$ and $\hat{q}_2$ are actually independent, it is not always true that $\mathcal{C}_1\lambda_1\hat{q}_2=\mathcal{C}_2\lambda_2\hat{q}_1$, but it can be regarded as an additional constraint.

(2) The fixed point set of R is given by $\mathrm{Fix}(R) = \{\mathbf{x} \in \mathbb{R}^n : R(\mathbf{x}) = \mathbf{x}\}$.
(3) An orbit $o(\mathbf{x}_0) = \{\mathbf{x}(t; \mathbf{x}_0) : t \in \mathbb{R}\}$ is R-symmetric if $R(o(\mathbf{x}_0)) = o(\mathbf{x}_0)$.

The system (23) with $j = 1$ can be written in the autonomous form (26) with

$$\mathbf{x} = (t, \theta_1, \dot{\theta}_1), \quad \mathbf{F}(\mathbf{x}) = \left(1, \dot{\theta}_1, -\frac{\lambda_1}{2}\left(\frac{a}{r(t;e)}\right)^3 \sin(2\theta_1 - 2f(t;e))\right). \tag{27}$$

One can easily check that each transformation defined by

$$R_{\alpha,\beta}(\mathbf{x}) = (2\alpha - t, 2\beta - \theta_1, \dot{\theta}_1), \quad \text{with} \quad (\alpha, \beta) \in \pi\mathbb{Z} \times \frac{\pi}{2}\mathbb{Z}, \tag{28}$$

is a reversing symmetry of Eq. (26) with $\mathbf{F}$ as in (27) because

$$f(2\alpha - t; e) = 2\alpha - f(t; e), \quad r(2\alpha - t; e) = r(t; e).$$

The same is true replacing in (28) the quantities $\theta_1, \dot{\theta}_1$ by $\theta_2, \dot{\theta}_2$.

On the other hand, the spin–spin problem in its Hamiltonian formulation is given by (21), that can be written as (26) with

$$\mathbf{x} = (t, \theta_1, \theta_2, p_1, p_2), \quad \mathbf{F}(\mathbf{x}) = \left(1, \frac{p_1}{\mathcal{C}_1}, \frac{p_2}{\mathcal{C}_2}, -\partial_{\theta_1} W(t, \theta_1, \theta_2), -\partial_{\theta_2} W(t, \theta_1, \theta_2)\right). \tag{29}$$

Each transformation defined by

$$R_{\alpha,\beta_1,\beta_2}(\mathbf{x}) = (2\alpha - t, 2\beta_1 - \theta_1, 2\beta_2 - \theta_2, p_1, p_2), \quad \text{with}$$
$$(\alpha, \beta_1, \beta_2) \in \pi\mathbb{Z} \times \frac{\pi}{2}\mathbb{Z} \times \frac{\pi}{2}\mathbb{Z}, \tag{30}$$

is a reversing symmetry of Eq. (26).

In the following sections we are going to emphasize the study of orbits that are symmetric with respect to the mentioned reversing symmetries using the following lemma.

Lemma 2 (From Theorem 4.1 in Lamb and Roberts 1998) *An orbit of* (26) *is* R*-symmetric if, and only if, it intersects the fixed point set* $\mathrm{Fix}(R)$.

3 Periodic and Quasi-Periodic Solutions of the Keplerian Models

In this section we provide the definitions of spin–orbit and spin–spin resonances, giving some results on the existence of periodic orbits (Sect. 3.1) and KAM tori (Sect. 3.2).

3.1 The Spin–Orbit and Spin–Spin Resonances

The periodic solutions of the Keplerian models presented in the Sect. 2.3 correspond to resonances between the orbital motion and the spin motion. The expansion of the

potential in (8) contains much interesting information concerning such resonances. First, let us introduce the definition of spin–orbit resonances.

Definition 3 We say that the ellipsoid $\mathcal{E}_1$ is in a standard spin–orbit resonance of order $m : n$ with $m \in \mathbb{Z}$, $n \in \mathbb{Z}\backslash\{0\}$, if

$$\theta_1(t + 2\pi n) = \theta_1(t) + 2\pi m. \tag{31}$$

The associated resonant angle $\psi_1^{m:n}(t) = mt - n\theta_1(t)$ is a periodic function of period $2\pi n$. The same definition holds for $\mathcal{E}_2$.

Recalling that we have normalized the mean motion to unity, we remark that Definition 3 states that the ratio of the orbital period of $\mathcal{E}_j$ over its period of rotation is m/n, $n \neq 0$. Additionally, according to Definition 3, the resonance $m : n$, $n \neq 0$, is also of order $km : kn$, $k \in \mathbb{Z}\backslash\{0\}$, but the converse is not true in general. For example, with (31), the resonance $1 : 1$ is also of order $2 : 2$, but a resonance $2 : 2$ may not be of order $1 : 1$. We can say that the resonance $m : n$ is of higher order than the resonance $m' : n'$ if $m/n > m'/n'$. This will be denoted using the notation $m : n > m' : n'$.

Next, we introduce a different definition of spin–orbit resonance.

Definition 4 We say that the ellipsoid $\mathcal{E}_1$ is in a *balanced* spin–orbit resonance of order $m : 2$, $m \in \mathbb{Z}$, if

$$\theta_1(t + 2\pi) = \theta_1(t) + m\pi. \tag{32}$$

In this case, the resonant angle $\psi_1^{m:2}(t)$ is 2π-periodic. The same definition holds for $\mathcal{E}_2$.

Notice that the two notions (31) and (32) are not equivalent: (32) implies (31) for $m : 2$, but the converse is not true. Actually, note that a balanced $2k : 2$ resonance, with $k \in \mathbb{Z}$, is a spin–orbit resonance of order $k : 1$. This new definition was motivated by Beletskii and Lavrovskii (1975), where the solutions associated to the resonance $3 : 2$ of the spin–orbit problem [say, (23) with $j = 1$] were studied numerically. Basically, they found out that the solutions satisfying (31), but not (32), appear only for large values of λ_1 ($\gtrsim 1$), also, for a given point (e, λ_1) the solutions appear in multiplets, and finally, the corresponding resonant angles have large amplitudes ($|\psi_1^{3:2}(t)| \gtrsim 0.75$) (see Table 1) in Beletskii and Lavrovskii (1975). On the other hand, solutions that obey (32) exist for any point in the (e, λ_1)-plane, including large regions of uniqueness of solution and resonant angle with small amplitude. Note that such amplitude is a measure of the deviation of the solution with respect to the uniform rotation of angular velocity $\frac{3}{2}t$. In Definition 4 we generalize these two types of resonances for any order $m : 2$, since this let us determine the main resonances in the first orbital revolution.

From De Vogelaere (1958), for instance, we know that a good tool to study a differential equation that has some reversing symmetries is by studying the periodic orbits that are invariant under such transformations.

In the next proposition we provide some boundary conditions that characterize the symmetric orbits in spin–orbit resonances.

Proposition 5 *The following statements hold for the spin–orbit problem (23), with $j = 1$ (ellipsoid $\mathcal{E}_1$):*

(1) *Any $R_{\alpha,\beta}$-symmetric orbit, with $R_{\alpha,\beta}$ defined in (28), associated to a $m : n$ spin–orbit resonance is equivalent to a solution that satisfies the following Dirichlet conditions:*

$$\theta_1(\alpha) = \beta, \quad \theta_1(\alpha + n\pi) = \beta + m\pi, \tag{33}$$

with $\alpha \in \{0, \pi\}$ and $\beta \in \{0, \frac{\pi}{2}\}$ (four combinations). Moreover, such solution satisfies the following symmetry property $\theta_1(t) = 2\beta - \theta_1(2\alpha - t)$.

(2) *There are two independent types of $R_{\alpha,\beta}$-symmetric orbits representing a balanced $m : 2$ spin–orbit resonance and are given by:*

$$\text{Type } 0 : \theta_1(0) = 0, \quad \theta_1(\pi) = \frac{m\pi}{2}, \tag{34}$$

$$\text{Type } \frac{\pi}{2} : \theta_1(0) = \frac{\pi}{2}, \quad \theta_1(\pi) = \frac{(m+1)\pi}{2}. \tag{35}$$

Moreover, the corresponding symmetry relations are: $\theta_1(t) = -\theta_1(-t)$ for type I and $\theta_1(t) = \pi - \theta_1(-t)$ for type II.

The same is true for (23), with $j = 2$ (ellipsoid $\mathcal{E}_2$), and also for (25).

Proof Let us apply Lemma 2 to (26) with $\mathbf{F}(\mathbf{x})$ given by (27). The fixed point set of each reversing symmetry $R_{\alpha,\beta}$ is $\text{Fix}(R_{\alpha,\beta}) = \{(t, \theta_1, \dot{\theta}_1) : t = \alpha, \theta_1 = \beta\}$, then the symmetric orbits can be found with initial conditions $\theta_1(\alpha) = \beta$. Since $\mathbf{F}(\mathbf{x})$ is 2π-periodic in t and π-periodic in θ_1, it is enough to consider $\alpha \in \{0, \pi\}$ (the periapsis and the apoapsis) and $\beta \in \{0, \frac{\pi}{2}\}$.

Now, since $R_{\alpha,\beta}$ is a reversing symmetry, if $\theta_1(t)$ is a solution of (23) with $j = 1$, so it is $\psi(t) = 2\beta - \theta_1(2\alpha - t)$. Additionally, if $\theta_1(\alpha) = \beta$, then both solutions coincide, so the symmetry relation $\theta_1(t) = 2\beta - \theta_1(2\alpha - t)$ holds for it. Now, if $\theta_1(t)$ is in a $m : n$ spin–orbit resonance, then replacing $t = \alpha - n\pi$ in (31), we get

$$\theta_1(\alpha + n\pi) = \theta_1(\alpha - n\pi) + 2\pi m.$$

From the symmetry relation we get additionally that

$$\theta_1(\alpha - n\pi) = 2\beta - \theta_1(\alpha + n\pi).$$

Combining the two expressions we prove (33).

Now let us prove the converse, that a solution $\theta_1(t)$ satisfying the conditions (33) is in $m : n$ spin–orbit resonance. Let the initial conditions of such solution be

$$\theta_1(\alpha + n\pi) = \beta + m\pi, \quad \dot{\theta}_1(\alpha + n\pi) = \tilde{\beta}, \tag{36}$$

for some real constant $\tilde{\beta}$. Since $\theta_1(\alpha) = \beta$, the solution has the symmetry relations $\theta_1(t) = 2\beta - \theta_1(2\alpha - t)$ and $\dot{\theta}_1(t) = \dot{\theta}_1(2\alpha - t)$. Using such relations we get that

$$\theta_1(\alpha - n\pi) = \beta - m\pi, \quad \dot{\theta}_1(\alpha - n\pi) = \tilde{\beta}. \tag{37}$$

The initial conditions (36) and (37) show that, while the time increases $2\pi n$, the angle θ_1 increases in $2\pi m$, and the angular velocity is the same for both cases, then the solution is periodic. With this, we have proved item 1.

Let us now consider the balanced $m : 2$ case in item 2. Note that, using the definition (32) instead of (31), we can follow the same procedure as before to prove that a balanced $m : 2$ solution satisfies the following boundary conditions

$$\theta_1(\alpha) = \beta, \quad \theta_1(\alpha \pm \pi) = \beta \pm \frac{m\pi}{2}, \tag{38}$$

and the symmetry relation $\theta_1(t) = 2\beta - \theta_1(2\alpha - t)$. Then, we get that the four types are in this case (34), with $\alpha = 0$, $\beta = 0$; (35), with $\alpha = 0$, $\beta = \pi/2$;

$$\text{Type } 0' : \theta_1(0) = -\frac{m\pi}{2}, \quad \theta_1(\pi) = 0,$$

with $\alpha = \pi$, $\beta = 0$, and

$$\text{Type } \frac{\pi}{2}' : \theta_1(0) = \frac{(1-m)\pi}{2}, \quad \theta_1(\pi) = \frac{\pi}{2},$$

with $\alpha = \pi$, $\beta = \pi/2$. Since an ellipsoid has a mirror symmetry with respect to any plane containing a pair of semi-axes, the angle θ_1 is equivalent to $\theta_1 + k\pi$, $k \in \mathbb{Z}$. In consequence, if $m = 2k_1, k_1 \in \mathbb{Z}$, type $0'$ is equivalent to type 0 and type $\frac{\pi}{2}'$ is equivalent to type $\frac{\pi}{2}$. Likewise, for $m = 2k_2 + 1, k_2 \in \mathbb{Z}$, type $0'$ is equivalent to type $\frac{\pi}{2}$ and type $\frac{\pi}{2}'$ is equivalent to type 0. Then, for resonances of order $m : 2, m \in \mathbb{Z}$, we will take types 0 and $\frac{\pi}{2}$ as representatives. With this, we have proved item 2.

The previous facts rely only on the symmetries and the periodicity of Eq. (23), including the discussion in Celletti and Chierchia (2000). Since Eq. (25) for the spin motion of $\mathcal{E}_1$, with $\mathcal{E}_2$ spherical, has exactly the same properties, then the proof above is also valid in such case. □

Proposition 5 let us characterize all the balanced spin–orbit resonances in the first half of an orbital revolution, additionally, the corresponding solutions have a certain symmetry relation. In the generalization to spin–spin resonances, we want to combine different spin–orbit resonances and we will use the boundary conditions in the same time interval.

Remark 6 Note that solutions of type $\frac{\pi}{2}$ can be recovered with the conditions of type 0 by considering negative values of λ_1. More precisely, solutions of type $\frac{\pi}{2}$ of Eq. (23) with $\lambda_1 = \lambda_* > 0$ are equivalent to solutions of (23) with $\lambda_1 = -\lambda_*$ satisfying conditions of type 0. The same holds for (25).

Remark 7 Proposition 5 gives a way to numerically search for balanced resonances. Indeed, Eqs. (34) and (35) can be used to apply a Newton method, that is, to find the initial condition $\dot{\theta}_1(0)$ such that the conditions for either Type 0 or Type $\frac{\pi}{2}$ are satisfied.

Next we introduce the following definition, which deals with the spins of both objects.

Definition 8 We say that the ellipsoids $\mathcal{E}_1, \mathcal{E}_2$ are in a standard spin–spin resonance[3] of order $(m_1 : n_1, m_2 : n_2)$ with $m_1, m_2 \in \mathbb{Z}, n_1, n_2 \in \mathbb{Z}\backslash\{0\}$, if the ellipsoid $\mathcal{E}_j$ is in a $m_j : n_j$ spin–orbit resonance. In such case, the resonant angles $\psi_{m_2:n_2}^{m_1:n_1}(t) = \psi_1^{m_1:n_1}(t) \pm \psi_2^{m_2:n_2}(t)$ are $2\pi n$-periodic functions, where n is the least common multiple of n_1 and n_2.

An analogous definition holds for resonances of the balanced type.

Definition 9 We say that the ellipsoids $\mathcal{E}_1, \mathcal{E}_2$ are in a balanced spin–spin resonance of order $(m_1 : 2, m_2 : 2)$ with $m_1, m_2 \in \mathbb{Z}$, if the ellipsoid $\mathcal{E}_j$ is in a $m_j : 2$ spin–orbit resonance for $j = 1, 2$.

Note that a spin–spin resonance of order $(m_1 : n_1, m_2 : n_2)$ is also of order $(\kappa_1 m_1 : n, \kappa_2 m_2 : n)$, where $n = \kappa_1 n_1 = \kappa_2 n_2$ is the least common multiple of n_1 and n_2. Again, the converse is not true in general. For example, the resonance $(1 : 1, 3 : 2)$ is of order $(2 : 2, 3 : 2)$, but not the opposite. However, a balanced resonance $(2 : 2, 3 : 2)$ is a spin–spin resonance of order $(1 : 1, 3 : 2)$.

The following proposition generalizes Proposition 5 to the spin–spin problem.

Proposition 10 *The following statements hold for the spin–spin problem (24):*

(i) *Any $R_{\alpha,\beta_1,\beta_2}$-symmetric orbit, with $R_{\alpha,\beta_1,\beta_2}$ defined in (30), associated to a $(m_1 : n, m_2 : n)$ spin–orbit resonance is equivalent to a solution that satisfies the following Dirichlet conditions:*

$$\theta_j(\alpha) = \beta_j, \quad \theta_j(\alpha + n\pi) = \beta_j + m_j\pi,$$

with $\alpha \in \{0, \pi\}$ and $\beta_j \in \{0, \frac{\pi}{2}\}$ (eight combinations). Moreover, such solution satisfies the following symmetry property $\theta_j(t) = 2\beta_j - \theta_j(2\alpha - t)$.

(ii) *There are four independent types of $R_{\alpha,\beta_1,\beta_2}$-symmetric orbits representing a balanced $(m_1 : 2, m_2 : 2)$ spin–spin resonance and are given by:*

$$\text{Type } (\beta_1, \beta_2) : \theta_j(0) = \beta_j, \quad \theta_j(\pi) = \beta_j + \frac{m_j\pi}{2}, \tag{39}$$

with $\beta_j \in \{0, \frac{\pi}{2}\}$. Moreover, the corresponding symmetry relation is $\theta_j(t) = 2\beta_j - \theta_j(-t)$.

[3] We remark that this is a practical definition because it is useful for the physical interpretation. However, we notice that there is a more general definition given by the resonant combination $n_0 t - n_1\theta_1 - n_2\theta_2$, with n_0, n_1, n_2 integers.

Proof This proof is based on the fact that the same arguments used to prove Proposition 5 can be generalized in a straightforward way for the spin–spin problem (24).

Now we apply Lemma 2 to (26) with $\mathbf{F}(\mathbf{x})$ given by (29). The fixed point set of each reversing symmetry $R_{\alpha,\beta_1,\beta_2}$ is

$$\mathrm{Fix}(R_{\alpha,\beta_1,\beta_2}) = \{(t, \theta_1, \theta_2, p_1, p_2) \colon t = \alpha, \theta_1 = \beta_1, \theta_2 = \beta_2\}.$$

Then, due to the periodicity of W in (20), the periodic orbits can be found at $\theta_j(\alpha) = \beta_j$, where we can take any combination between $\alpha \in \{0, \pi\}$ and $\beta_j \in \{0, \frac{\pi}{2}\}$. A similar method was used in Greene (1979) for the standard map and was generalized for the spin–orbit problem in Celletti and Chierchia (2000) and for a standard map of two degrees of freedom in Celletti et al. (2004).

The rest of the proof of item i follows analogously to the proof of item (1) of Proposition 5 using the reversing symmetries.

The proof of item ii needs more detail. In the same way as (38), we obtain easily that the balanced resonances $(m_1 : 2, m_2 : 2)$ are given by

$$\theta_j(\alpha) = \beta_j, \quad \theta_j(\alpha \pm \pi) = \beta_j \pm \frac{m_j \pi}{2}. \tag{40}$$

We see that (39) corresponds to (40) with $\alpha = 0$ and the positive sign. From the case $\alpha = \pi$ and the negative sign, we have that

$$\theta_j(0) = \beta_j - \frac{m_j \pi}{2}, \quad \theta_j(\pi) = \beta_j. \tag{41}$$

Note that if, for example, we take $j = 1$ and $m_1 = 2k_1$, with $k_1 \in \mathbb{Z}$, then the conditions (39) and (41) are equivalent. On the other hand, if $m_1 = 2k_1 + 1$, then the conditions (39) with $\beta_1 = 0$ and $\frac{\pi}{2}$ are equivalent respectively to (41) with $\beta_1 = \frac{\pi}{2}$ and 0. The same is true for $j = 2$. Then, with (39) all the possibilities are covered. □

Remark 11 Results in Proposition 10 allow to apply a Newton method to compute resonances for the spin–spin problem just considering as unknowns $\dot{\theta}_j(0)$ and correct them by imposing the conditions in (39) or (41).

For circular orbits ($e = 0$), each of the spin–orbit models (23) is a classical pendulum whose only stable equilibrium point corresponds to a $1 : 1$ resonance that is given by $\theta_j(t) = t$. Similarly, the spin–spin model (24) consists of two coupled penduli whose only stable solution is $\theta_1(t) = \theta_2(t) = t$ that is a $(1 : 1, 1 : 1)$ resonance. However, for $e \neq 0$, $f(t; e)$ does not coincide with t and more stable spin–orbit resonances may appear.

In order to study the spin–orbit and spin–spin resonances, it is useful to compute the expansion of V_2 and V_4 up to some power of the eccentricity. This expansion is obtained solving Kepler's equation (13) up to a finite order in the eccentricity, then inserting the solution $u = u(t)$ in (14), (16), expand them in series of the eccentricity and finally expanding the trigonometric terms appearing in (8).

This procedure leads to the expansions of V_2 and V_4 that, for simplicity, we give up to the order 2 in the eccentricity in "Appendix C." In those expressions,

Table 1 Resonances appearing in the expansion of the potential $V_2 + V_4$ for each order of the eccentricity

Order	Spin–orbit resonances		Spin–spin resonances
	V_2	V_4	V_4
e^0	1 : 1	1 : 1	Combine 1 : 1 with 1 : 1
e^1	3 : 2, 1 : 2	3 : 2, 1 : 2, 3 : 4, 5 : 4	Combine 1 : 1 with 3 : 2 and 1 : 2
e^2	1 : 1, 2 : 1, 0 : 1	1 : 1, 2 : 1, 0 : 1	Combine 1 : 1 with 1 : 1, 2 : 1 and
		0 : 1, 1 : 2, 3 : 2	All combinations between 3 : 2 and 1 : 2

the trigonometric terms with arguments $\psi_j^{m_j:n_j}(t) = m_j t - n_j\theta_j$ are associated to $m_j : n_j$ spin–orbit resonances for $\mathcal{E}_j$, whereas the terms with argument $\psi_{m_2:n_2}^{m_1:n_1}(t) = (m_1 \pm m_2)t - n_1\theta_1(t) \mp n_2\theta_2(t)$ correspond to spin–spin resonances by combining spin–orbit resonances of orders $m_1 : n_1$ and $m_2 : n_2$. For each order of the expansion in the eccentricity e, there are some resonances appearing. They are shown in Table 1, where we can recognize a hierarchy: the most important spin–orbit resonance is 1 : 1, then we have 3 : 2, 1 : 2 and so on, because they appear for low orders of the eccentricity. Resonances of further orders are relevant only for large eccentricities.

Note that the most relevant spin–orbit resonances are of order $m : 2, m \in \mathbb{Z}$. Additionally, spin–spin resonances appearing at order e^α in V_4 are obtained by combining spin–orbit resonances appearing at order e^{α_1} and e^{α_2} in V_2 such that $\alpha_1 + \alpha_2 = \alpha$.

Finally, note that for V_2, the coefficients associated to spin–orbit resonances are of order one in d_1, d_2, whereas for V_4, the spin–orbit coefficients are of order two in d_1, d_2, q_1, q_2, and the spin–spin coupling coefficients are of order two in d_1, d_2.

3.2 KAM Tori in the Spin–Spin Problem

Now we deal with quasi-periodic solutions of the Keplerian version of the spin–spin model. We denote by

$$\underline{\omega} = (1, \omega_1, \omega_2) \tag{42}$$

the frequency vector with

$$\omega_1 = \frac{p_1}{C_1}, \quad \omega_2 = \frac{p_2}{C_2}.$$

The Hessian matrix associated to (20) has determinant different from zero, whenever $p_1 \neq 0$, $p_2 \neq 0$. This implies that (20) satisfies the Kolmogorov non-degeneracy condition, which is a requirement for the applicability of KAM theorem (Kolmogorov 1954; Arnol'd 1963; Moser 1962). The other essential requirement in KAM theory is the assumption that the frequency satisfies a Diophantine inequality, namely there exist $C > 0$ and $\xi \geq 2$, such that

$$|\underline{k} \cdot \underline{\omega}|^{-1} \leq C|\underline{k}|^{\xi} \tag{43}$$

for $\underline{k} \in \mathbb{Z}^3 \setminus \{\underline{0}\}$.

We remark that a possible choice of $\underline{\omega}$ satisfying (43) can be obtained as follows. Let α be an algebraic number of degree 3, namely the solution of a polynomial equation of degree 3 with integer coefficients, not being the root of polynomial equations of lower degree. Let us consider the vector $\underline{\omega} = (1, \omega_1, \omega_2)$ obtained as

$$\begin{pmatrix} 1 \\ \omega_1 \\ \omega_2 \end{pmatrix} = \begin{pmatrix} 1 & 0 & 0 \\ b_1 & a_{11} & a_{12} \\ b_2 & a_{21} & a_{22} \end{pmatrix} \begin{pmatrix} 1 \\ \alpha \\ \alpha^2 \end{pmatrix}, \tag{44}$$

where (b_1, b_2) and the matrix $A \equiv (a_{mn})$ have rational coefficients and $\det A \neq 0$. By number theory results (see, e.g., Celletti et al. 2004), a vector $\underline{\omega}$ as in (44) satisfies (43) with $\xi = 2$. Under smallness conditions of the parameters, say λ_j in (22), KAM theory ensures the existence of a quasi-periodic torus with Diophantine frequency. We remark that the theory presented in Calleja et al. (2022b) for the spin–orbit problem (see also Calleja et al. 2022a, c) can be extended to provide explicit estimates for (20) and an explicit algorithm to construct quasi-periodic solutions.

4 Qualitative Description of the Spin Models

In this section, we give a qualitative description of the phase space associated to the spin–orbit problem (Sect. 4.1), the spin–spin problem with spherical companion (Sect. 4.2) and with non-spherical companion (Sect. 4.3).

4.1 Spin–Orbit Problem ($V_{\text{per}} = V_2$)

Since the system (23) corresponds to two uncoupled spin–orbit problems, then the Poincaré map of the whole system can be understood as the direct product of the Poincaré maps for each of the bodies. Consider for example the dynamics of $\mathcal{E}_1$. Figure 3 is a typical Poincaré map of the spin–orbit problem obtained using a Taylor integrator (Jorba and Zou 2005) and using a similar approach as the one explained in "Appendix B," in this case with parameters $(e, \lambda_1) = (0.06, 0.05)$; it represents solutions at $t = 2\pi k, k \in \mathbb{Z}$, in the plane $(\theta_1, \dot{\theta}_1)$ restricted to $\theta_1 \in [-\pi, \pi]$. The main stable resonances are tagged with their corresponding order $m : n$. The Poincaré map for sufficiently small parameters (e, λ_1) has the following features:

(1) The main stable spin–orbit resonances are represented by fixed points in the plane $(\theta_1, \dot{\theta}_1)$ surrounded by islands of invariant librational tori. High order resonances appear above low order resonances.
(2) It looks that the spin–orbit resonances of order $m : 2 \geq 1 : 1$ are balanced: solutions of type 0 (34) are stable and those of type $\frac{\pi}{2}$ (35) are unstable. On the contrary, for the $1 : 2$ resonance, type 0 is unstable and type $\frac{\pi}{2}$ is stable. Concerning other resonances (33), for instance in the $3 : 4$ resonance, types with $\alpha = 0$ are unstable and types with $\alpha = \pi$ are stable. Exactly the opposite occurs for the case $5 : 4$.

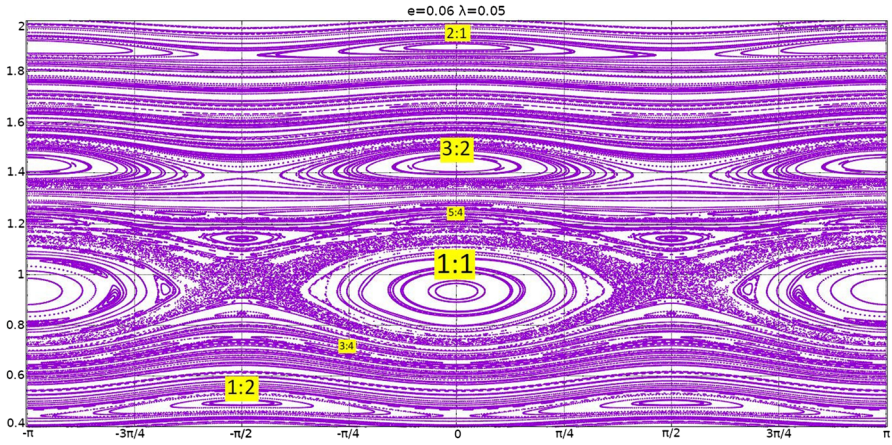

Fig. 3 Poincaré map for the spin–orbit problem

(3) It is possible to have stable secondary resonances, namely small resonances surrounding other resonances. This is clear for the $1:1$ resonance. Beyond the librational islands associated to the resonance $1:1$, there is a chaotic region that includes the unstable resonances and that is larger for large parameters (e, λ_1). The chaotic region can appear for other resonances and is limited by rotational tori that also distinguish the domains of resonances of different orders.

4.2 Spin–Spin Problem ($V_{\text{per}} = V_2 + V_4$) with Spherical Companion

Let us now consider the case when $\mathcal{E}_2$ is a sphere. Then, $\theta_2(t) = \theta_2(0) + \dot{\theta}_2(0)t$ and the dynamics of θ_1 is given by (25), that depends on the parameters $(e, \lambda_1, \hat{q}_1, \sigma_1)$. Here the parameters σ_1 and $\hat{q}_1$ perturb the previous framework of the spin–orbit problem (see Sect. 4.1). We can see a comparison between both problems in Fig. 4: we see that the only qualitative difference between both cases is that the Poincaré map associated to Eq. (25) is slightly more chaotic. This minor difference is due to the fact that we take $\sigma_1 = \hat{q}_1 = 0.01$, that are small parameters. As we will see in Sect. 6, the spin–spin model is a good approximation for the dynamics of two ellipsoids for σ_j and $\hat{q}_2$ up to the order of magnitude of about 10^{-2}, because larger values could lead to a collision (see Sect. 6.2).

4.3 Spin–Spin Problem ($V_{\text{per}} = V_2 + V_4$) with Non-spherical Companion

Now we deal with the general system (24). Let $\Psi(t) = (\theta_1(t), \theta_2(t), \dot{\theta}_1(t), \dot{\theta}_2(t))$ be a solution of (24) and its respective projections $\Psi_1(t) = (\theta_1(t), \dot{\theta}_1(t))$ and $\Psi_2(t) = (\theta_2(t), \dot{\theta}_2(t))$. From now on we restrict $\theta_j(t)$ to $[-\pi, \pi]$. Let the Poincaré map associated to such solution be defined by $\mathcal{P}(\Psi(0)) = \Psi(2\pi)$, and its projections by $\mathcal{P}_j(\Psi_j(0)) = \Psi_j(2\pi)$. It is not possible to represent the iteration of the map $\mathcal{P}$ in a single plot, because it is 4-dimensional, so we will represent the projections

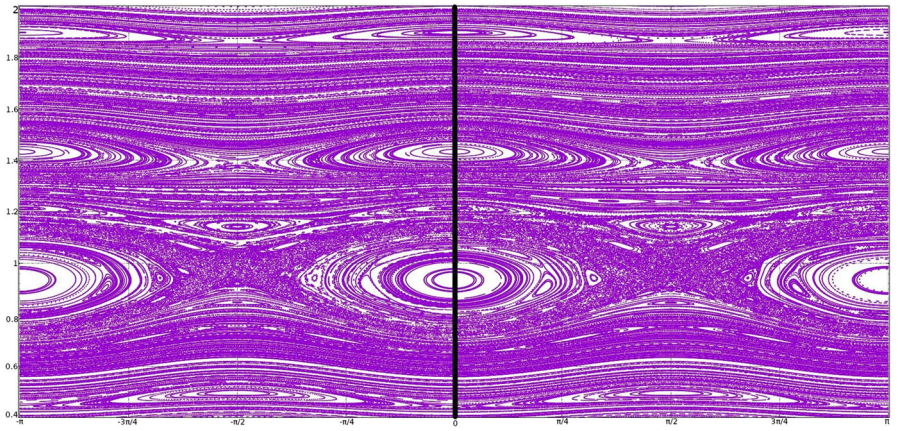

Fig. 4 Poincaré maps. Left: usual spin–orbit problem with $(e, \lambda_1) = (0.06, 0.05)$. Right: spin–orbit problem up to order $1/r^5$ with $(e, \lambda_1, \sigma_1, \hat{q}_1) = (0.06, 0.05, 0.01, 0.01)$

$\mathcal{P}_j$. That is to say, for a solution $\Psi(t)$, we are interested in the behavior of the two families of points $\Psi_1(2\pi k)$ and $\Psi_2(2\pi k)$, $k \in \mathbb{Z}$, in a single 2-dimensional strip $\Pi = \{(x, y) \in \mathbb{R}^2 \colon |x| \leq \pi\}$. We recognize the following features:

(1) A solution in spin–spin resonance corresponds to a family of isolated recurrent points of $\mathcal{P}$ (namely, the successive points on the Poincaré map), whose projections are represented in Π as a pair of families of recurrent points.
(2) If the spin–spin resonance is stable, then nearby solutions would librate around such points. While in the uncoupled system, librating solutions belong to 2-dimensional tori, here tori can be higher dimensional. As a result, the projected points represented in Π are distributed in two clouds of points surrounding each recurrent point. A cloud of this kind covers an annulus-like region of a certain thickness that is usually thicker for stronger couplings. A similar behavior occurs for rotational solutions, whose corresponding clouds are distributed in strips of certain thickness, see Fig. 5.
(3) We expect that, for small enough coupling parameters σ_j, the spin–spin resonances are located close to the corresponding spin–orbit resonances for each ellipsoid, and would keep the same stability as for the uncoupled problem. However, we have found that, for larger σ_j, the stability may change with respect to the uncoupled system (see Fig. 6).
(4) The coupled system is 5-dimensional; then, invariant tori, if there exist, would not confine solutions in determined regions (as in the uncoupled system), but Arnold diffusion is expected to take place.

A particular behavior occurs only when both bodies are identical ($\mathcal{C}_1 = \mathcal{C}_2 = 0.5$, $\lambda = \lambda_1 = \lambda_2, \sigma = \sigma_1 = \sigma_2$ and $\hat{q} = \hat{q}_1 = \hat{q}_2$), the so-called *measure synchronization*. This phenomenon was observed numerically in Hampton and Zanette (1999) for an autonomous Hamiltonian system of two degrees of freedom (a pair of identical coupled oscillators): the system librates around a stable periodic solution in a very particular way described as follows for our system (see the phenomenon illustrated in Fig. 7).

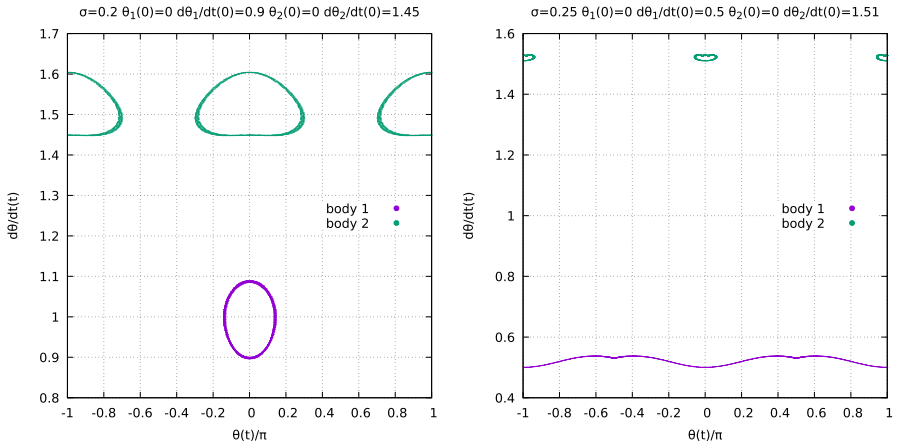

Fig. 5 Left: Projections $\Psi_1(2\pi k)$ and $\Psi_2(2\pi k)$, $k \in \mathbb{N}$ of a solution $\Psi(2\pi k)$ librating around a stable $(1:1, 3:2)$ spin–spin resonance. Right: solution for which one of the bodies librates around a stable spin–orbit resonance and the other one has a rotational behavior. The common parameter values are $e = 0.06$, $\lambda_1 = \lambda_2 = 0.05$, and $\hat{q}_1 = \hat{q}_2 = 0.001$

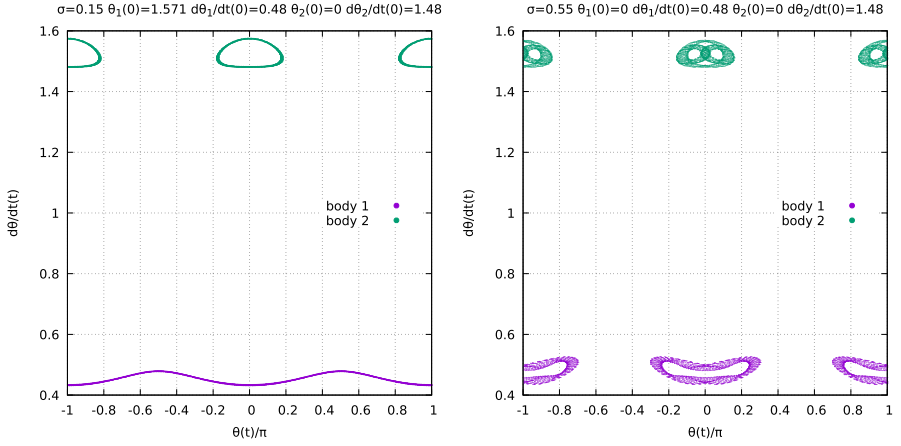

Fig. 6 Left: Projections $\Psi_1(2\pi k)$ and $\Psi_2(2\pi k)$, $k \in \mathbb{Z}$ of a solution $\Psi(t)$ close to an unstable $(1:2, 3:2)$ spin–spin resonance. Right: Representation of a solution with identical $\Psi(0)$ for larger coupling, now the nearby spin–spin resonance has become stable. The common parameter values are $e = 0.06$, $\lambda_1 = \lambda_2 = 0.05$, and $\hat{q}_1 = \hat{q}_2 = 0.001$

Take a solution $\Psi(t)$ librating around a stable spin–spin resonance of order $(m:n, m:n)$. Consider the two families of points $\Psi_1(2\pi k)$ and $\Psi_2(2\pi k)$ and their corresponding annulus-like region in the plane Π. There are two possibilities: either both clouds of points are distributed in separated annulus-like regions or both regions coincide. That is to say, either the overlap is empty or there is a complete overlap. Moreover, if we start with a solution with separated regions, we can obtain the complete overlap by increasing the coupling parameter σ (keeping the same $\Psi(0)$). The phenomenon takes place suddenly for a specific $\sigma = \sigma_*$ when the outer boundary of the inner ring

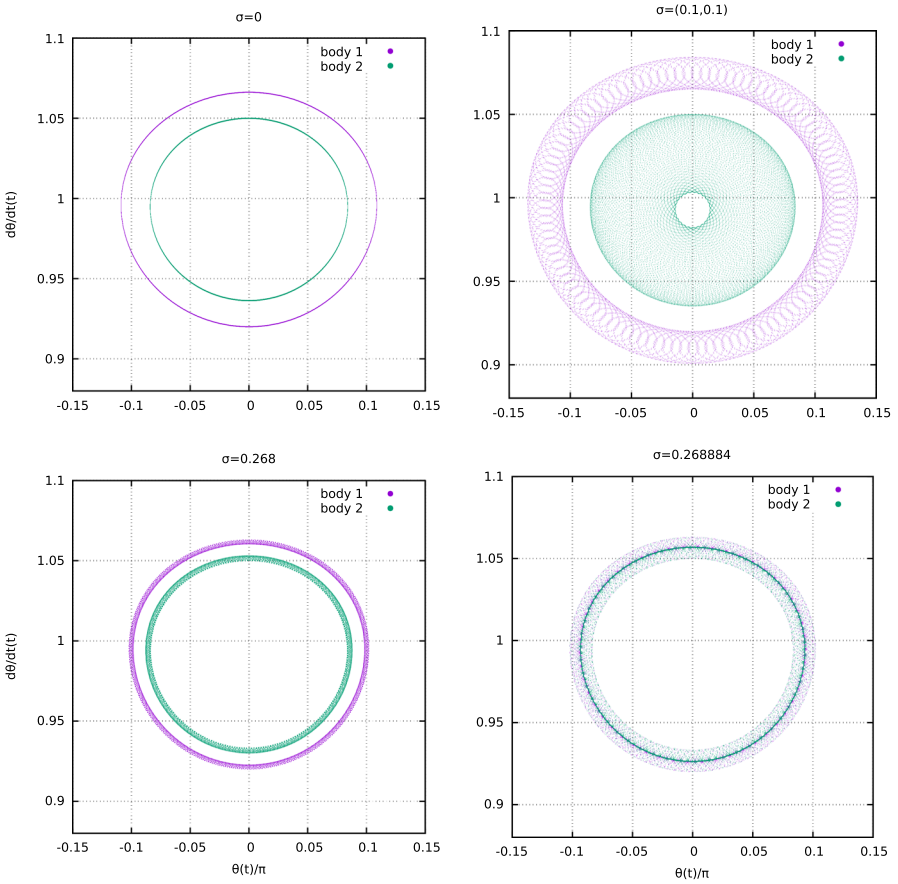

Fig. 7 Projections $\Psi_1(2\pi k)$ and $\Psi_2(2\pi k)$, $k \in \mathbb{Z}$ of a solution $\Psi(t)$ close to a stable $(1:1, 1:1)$ spin–spin resonance for different values of σ_1 and σ_2. Keeping the same parameters $e = 0.06$, $\lambda_1 = \lambda_2 = 0.05$, $\hat{q}_1 = \hat{q}_2 = 0.001$, $\theta_1(0) = \theta_2(0) = 0$, $\dot{\theta}_1(0) = 0.92$ and $\dot{\theta}_2(0) = 1.05$. The external ring (body 1) keeps similar thickness, the internal ring changes from a thin one to another that occupies values close to $(0, 0)$ to thin one to finally collapse with the exterior one

touches the inner boundary of the outer ring. At that moment, there is a concentration of density of points in the contact region.

The phenomenon of measure synchronization disappears when the bodies are not equal. See in Fig. 8 how the domains of both ellipsoids can overlap without merging into a single ring.

5 Linear Stability of Resonances

In this section we analyze the stability (in the linear approximation) of solutions associated to the resonances in different models, namely the spin–orbit problem (Sect. 5.1)

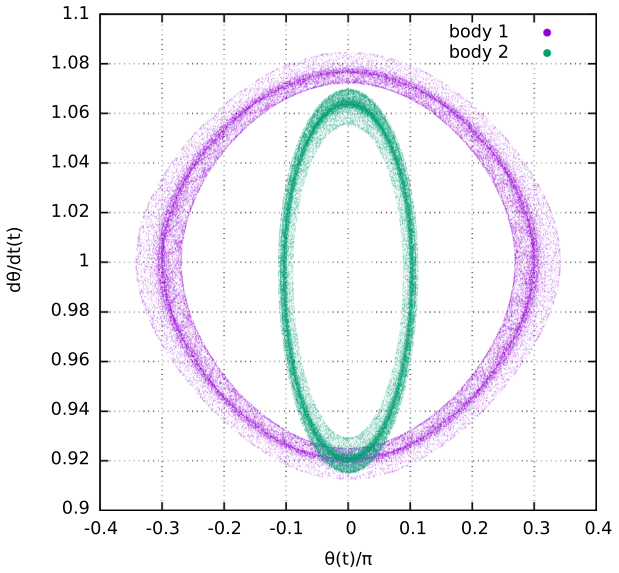

Fig. 8 Partial overlapping of the domains of $\Psi_1(2\pi k)$ and $\Psi_2(2\pi k)$, $k \in \mathbb{Z}$ of a solution $\Psi(t)$ close to a stable $(1:1,1:1)$ spin–spin resonance in the case of different bodies: no measure synchronization. The parameter values are $e = 0.06$, $\lambda_1 = 0.009$, $\lambda_2 = 0.05$, $\hat{q}_1 = \hat{q}_2 = 0.001$, $\sigma_1 = \sigma_2 = 0.3$, $\theta_1(0) = \theta_2(0) = 0$, $\dot{\theta}_1(0) = 0.92$, and $\dot{\theta}_2(0) = 1.064$

and the spin–spin problem with spherical (Sect. 5.2) and non-spherical (Sect. 5.3) companion.

In all cases, we will only deal with balanced resonances (32), because they appear to be simpler and more relevant (see Sect. 4) than resonances of the general type (31). Actually, we can establish regions in the space of parameters where solutions associated to balanced resonances are unique or have some low multiplicity. In the case of the spin–spin problem, we restrict ourselves to regions of uniqueness. The study of linear stability of such periodic solutions in the space of parameters complements the understanding of the dynamics that we presented in previous sections, especially Sect. 4.

5.1 Spin–Orbit Problem ($V_{\mathbf{per}} = V_2$)

Consider the spin–orbit problem (23) with $j = 1$, that is, the motion of the ellipsoid $\mathcal{E}_1$. Let $\theta_1 = \theta^*(t)$ be a solution in a balanced $m : 2$ spin–orbit resonance, whose associated variational equation is

$$\ddot{y} + \lambda_1 \left(\frac{a}{r(t;e)} \right)^3 \cos(2\theta^*(t) - 2f(t;e))y = 0, \quad y \in \mathbb{R}. \tag{45}$$

For $e \neq 0$, (45) is a linear equation with a 2π-periodic coefficient. Particularly, this is a Hill's equation (Magnus and Winkler 1979). Assume that $\Phi(t)$ is a matrix solution of (45) with $\Phi(t_0) = \mathbb{1}_2$, the identity matrix 2×2. The stability of (45) is determined by

the structure of the matrix $M = \Phi(t_0 + 2\pi)$, called monodromy matrix. If $|\operatorname{Tr}(M)| < 2$, we have elliptic stability, whereas if $|\operatorname{Tr}(M)| > 2$ we have hyperbolic instability. In the parabolic case, when $|\operatorname{Tr}(M)| = 2$, the system is stable if the Jordan canonical form of M is $\mathbb{1}_2$ or $-\mathbb{1}_2$, otherwise the system is unstable. Actually, if the system is parabolic unstable, the instability of the linear system is linear in time, but hyperbolic instability is associated to an exponential divergence in time. In our case, we want to distinguish regions of stability and instability in the (e, λ_1)-plane for a given solution, which is continuous in (e, λ_1). From properties of Hill's equations, regions of elliptic stability are separated from regions of hyperbolic instability by parabolic curves ($|\operatorname{Tr}(M)| = 2$). These curves are made of unstable points, except if there are intersections of parabolic curves, because points of intersection become stable. This phenomenon is called *coexistence*, Magnus and Winkler (1979).

For a given point (e, λ_1) and a given balanced $m : 2$ resonance, we want to know how many solutions there are of each type (34) or (35), and their linear stability. First, recall Remark 6: solutions of type $\frac{\pi}{2}$ satisfy conditions of type 0 for the equation (23) with $j = 1$, taking $-\lambda_1$ instead of λ_1. Consequently, for each (e, λ_1), with $e \in [0, 1)$ and $\lambda_1 \in (-3, 3)$, we can obtain all the solutions corresponding to a balanced resonance by applying the shooting method: take a solution $\theta_1(t)$ with initial conditions[4] $\theta_1(\pi) = m\pi/2$, $\dot{\theta}_1(\pi) = \gamma \in \mathbb{R}$ and let γ vary until the boundary condition $\theta_1(0) = 0$ is reached. Finally, we obtain the linear stability of the solution by computing $\Phi(t)$ such that $\Phi(\pi) = \mathbb{1}_2$. Actually, for this procedure, we can take any of the boundary conditions in Eqs. (34) and (35), we just need one type to generate all solutions.

The results of this method for the main balanced spin–orbit resonances are shown in Fig. 9. For these computations, we used a Runge–Kutta Verner 8(9) integrator (Verner 1978), instead of a Taylor integrator (Jorba and Zou 2005); the reason is that, for some parameter values, the solutions are constant or polynomials and the Taylor method suffers in choosing a good step size. Thus, Fig. 9 requires around 3.5 days with 34 CPUs to be generated with a discretization mesh size of $2000 \times 2000 \times 2000$ for (e, λ_1, γ).

We can recognize the following characteristics[5]:

(1) Each of the balanced resonances is represented in the (e, λ_1, γ)-space by a continuous surface. In the case $1 : 1$, the surface is made of two sheets connected only in one point $(e, \lambda_1) = (0, 1)$.
(2) The region of uniqueness in the (e, λ_1)-plane is quite large. The multiplicity is generated by bifurcation of solutions: the surface folds generating multiple solutions (from one to three, as far as we see). Particularly, the bifurcation in the case $1 : 1$ occurs at $(e, \lambda_1) = (0, 1)$ producing a secondary sheet behind the main one. In general, the multiplicity takes place for some regions with $|\lambda_1| > 1$. The resonances of order $m : 2$ with $m > 2$, have two characteristic folds, one with a

[4] We choose to take initial conditions at $t = \pi$ and not $t = 0$ because the values of $\dot{\theta}_1(0)$ producing spin–orbit resonances for large e and λ_1 are too large to be represented in a 3-dimensional plot as in Fig. 9.

[5] The linear stability of the multiple solutions associated to the resonances $1 : 1$ and $3 : 2$ was already studied in Zlatoustov et al. (1966), Beletskii (1966) and Beletskii and Lavrovskii (1975), but we include them here in order to have a more complete view.

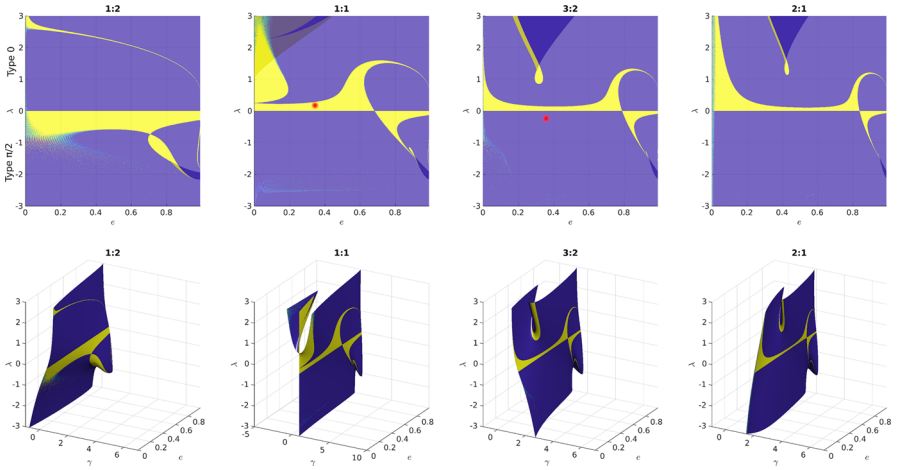

Fig. 9 Diagrams of linear stability for the balanced resonances of order $1:2$ (left), $1:1$ (middle left), $3:2$ (middle right) and $2:1$ (right). Blue-instability and yellow-stability. The upper diagrams are projections of the lower diagrams in the (e, λ_1)-plane with some transparency in order to identify regions with multiplicity of solutions (Color figure online)

V-like shape in solutions of type 0 for $\lambda_1 > 1$, and another small one in solutions of type $\frac{\pi}{2}$ for $\lambda_1 \sim -2$ and very large eccentricities.

(3) Instability is predominant in the diagrams, especially in solutions of type 0 for the resonance 1:2 and of type $\frac{\pi}{2}$ for the rest of the resonances. We see that the main regions of linear stability are continuation of stable solutions from $e = 0$, much of which are close to small $|\lambda_1|$. Except for the resonance $1:2$, the stability region for large eccentricities ($e > 0.6$) of the other resonances has a similar shape, characterized by a bifurcation with an interchange of stability. It is interesting to note that the folds producing the multiplicity are associated to some stable regions with peculiar shapes. In the resonance $1:1$ we find two unstable regions bifurcating from the exact solution $\theta_1(t) = t$ for $e = 0$: one at $\lambda_1 = 1/4 = 0.25$ (main sheet) and the other one at $\lambda_1 = 9/4 = 2.25$ (secondary sheet).

Now let us consider both bodies. Since the system (23) is uncoupled, then the multiplicity and stability associated to a spin–spin resonance is given by each of the separated problems. For example, take the $(1:1, 3:2)$ balanced spin–spin resonance of type $(0, \frac{\pi}{2})$ for $(e, \lambda_1, \lambda_2) = (0.3, 0.1, 0.5)$, that is, the red points shown in Fig. 9. It has associated a unique solution and it is unstable because it is so for θ_2.

5.2 Spin–Spin Problem ($V_{\text{per}} = V_2 + V_4$) with Spherical Companion

In this case we know that $\mathcal{E}_2$ is in uniform rotation $\theta_2(t) = \theta_2(0) + \dot{\theta}_2(0)t$, while the dynamics of θ_1 is given by (25), that depends on $(e, \lambda_1, \hat{q}_1, \sigma_1)$. For this problem, we can proceed in the same way as for the spin–orbit problem of Sect. 5.1. On one hand, the variational equation associated to a solution in a spin–orbit resonance is a Hill's equation like (45), so the linear stability of the solution is characterized by the

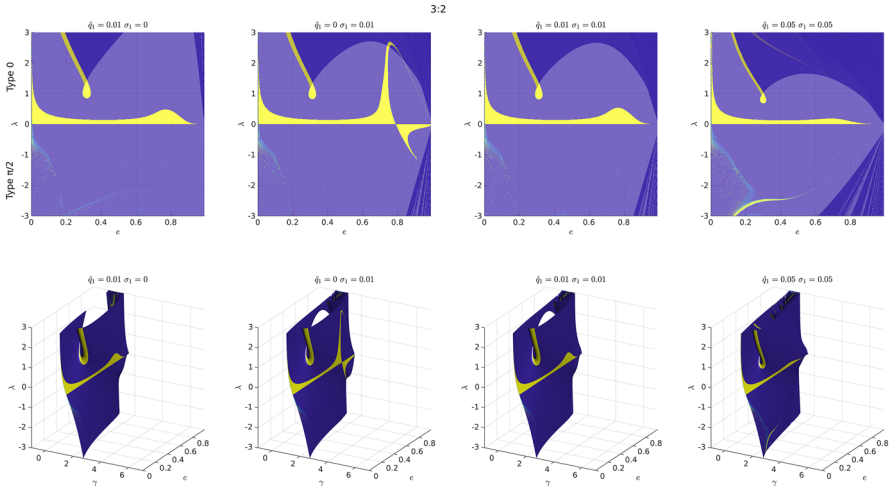

Fig. 10 Diagrams of linear stability for the 3 : 2 balanced resonance of (25) for different values of the indicated parameters $(\hat{q}_1, \sigma_1)$. Blue denotes instability and yellow denotes stability. Each of the columns has required around 15 h using 24 CPUs and a mesh size of $512 \times 512 \times 512$ (Color figure online)

corresponding monodromy matrix. On the other hand, we can find all the solutions associated to a balanced spin–orbit resonance using the shooting method for only one type of boundary conditions by including negative values of λ_1 (see Remark 6).

Comparing Figs. 9 and 10, we can see, for example, how the balanced 3 : 2 resonance is perturbed when we turn on the parameters $(\hat{q}_1, \sigma_1)$:

(1) The effect of the new parameters is remarkable for large e and $|\lambda_1|$. Especially when $\hat{q}_1$ and σ_1 are large.
(2) At very large eccentricities, the surface has a complicated structure resulting in multiple solutions. The effect of $\hat{q}$ is mainly to alter the stability for large e: solutions of type $\frac{\pi}{2}$ become always unstable, while stable regions of solutions of type 0 are more concentrated. The growth of $\hat{q}$ also increases the multiplicity of solutions of type 0 and very large e. On the other hand, increasing σ_1 has a more dramatic effect on the complexity of the surface and also modifies the stability for large e. Actually, for some values of σ_1, the existing V-shaped fold connects with the complex structure of large eccentricities in the upper part of the diagram.

5.3 Spin–Spin Problem ($V_{\text{per}} = V_2 + V_4$) with Non-spherical Companion

We study the linear stability of the resonances of the full coupled spin–spin model in (24). In this case, linear stability is determined by a more general theory and we will restrict ourselves to zones in the space of parameters where there is uniqueness.

Since we have two degrees of freedom, the first variation at a particular resonance is not a Hill's equation anymore, but a coupled system of second order. A Hill's equation is a particular case of linear Hamiltonian system with periodic coefficients, hereafter LPH systems.

If we define $z = (\theta_1, \theta_2, p_1, p_2)^{\mathsf{T}}$, where $p_j = \mathcal{C}_j \dot{\theta}_j$, the spin–spin problem in the Hamiltonian form (21) can be written as

$$\dot{z} = J_2 \partial_z H_K(t, z), \tag{46}$$

where J_l is the square matrix of order $2l$ given by

$$J_l = \begin{pmatrix} 0 & \mathbb{1}_l \\ -\mathbb{1}_l & 0 \end{pmatrix}, \quad l = 1, 2, \ldots \tag{47}$$

with $\mathbb{1}_l$ the unit matrix of order l. The non-autonomous Hamiltonian $H_K(t, z)$ is given in (19) for $V_{\text{per}} = V_2 + V_4$. Let $z = z^*(t)$ be a solution of (46) that is in a balanced spin–spin resonance of type $(m_1 : 2, m_2 : 2)$. Then, the first variation at such solution has the form

$$\dot{y} = J_2 \partial_{z,z} H_K(t, z^*(t)) y, \quad y \in \mathbb{R}^4, \tag{48}$$

where $\partial_{z,z} H_K$ denotes the Hessian matrix of the Hamiltonian H_K in the 4-dimensional variable z. The system (48) is an LPH system of period 2π. Assume that $\Phi(t)$ is a matrix solution of (48) with $\Phi(t_0) = \mathbb{1}_4$. The stability of (48) is determined by the Floquet multipliers, that are the eigenvalues of the monodromy matrix $\Phi(t_0 + 2\pi)$.

An LPH system has particular stability properties, see the general theory in Yakubovich and Starzhinskii (1975), Ekeland (1990) and an application to the double synchronous spin–spin resonance in Misquero (2021). For example, assume that $\varphi \in \mathbb{C}$ is a Floquet multiplier of an LPH system. Then, its inverse φ^{-1}, its complex conjugates $\bar{\varphi}$ and $\bar{\varphi}^{-1}$ are also multipliers and have the same multiplicity as φ. That is, the Floquet multipliers have a symmetric distribution with respect to the real line and the unit circle of the complex plane. In consequence, a necessary condition for stability is that all multipliers have modulus 1. Moreover, if all multipliers have modulus 1 and they are all different, then the system is stable. When all the multipliers have modulus 1 and some of them coincide, the situation is not trivial and the stability depends on further algebraic properties of the multipliers (Krein's theory, 1950). Then, unlike for Hill's equations, here we do not have a quantity like the trace of the monodromy matrix in order to characterize the boundary of stability/instability regions. Instead, we will use the following definition.

Definition 12 We will say that an LPH system is *hyperbolic unstable* if

$$\max_k |\varphi_k| > 1,$$

where φ_k, $k = 1, 2, \ldots$, are all the Floquet multipliers of the system.

Assume that the solution $z^*(t)$ is continuous in some domain of the parameters of the model $(e; \mathcal{C}_1, \lambda_1, \lambda_2, \sigma_1, \hat{q}_1, \hat{q}_2)$. The equation $\max_{k=1,\ldots,4} |\varphi_k| = 1 + \varepsilon$, with $\varepsilon > 0$, defines a 1-parametric family of hyperbolic unstable manifolds in the space of parameters; then, the boundary of hyperbolic instability will be found if we take the limit of such manifolds as $\varepsilon \to 0$.

On the other hand, it is possible to find all the solutions of a given type of a balanced spin–spin resonance using the shooting method as in the previous section. However, since the phase space and the space of parameters have large dimensions, our approach will be to obtain the solutions by continuation. Note that the solutions of (24) for $\lambda_j = 0$ and any $e \in [0, 1)$ are exactly given by $\theta_j(t) = \theta_j(0) + \dot{\theta}_j(0)t$. Then, the unique solution of type (β_1, β_2) of a balanced spin–spin resonance $(m_1 : 2, m_2 : 2)$ is just $\theta_j(t) = \beta_j + \frac{m_j}{2}t$. Such solution can be continued for $|\lambda_j| > 0$. For small enough $|\lambda_j|$, the systems in Eqs. (23) to (25) can be regarded as different perturbations of the system $\ddot{\theta}_j = 0$, and then Figs. 9 and 10 give us a quite clear idea of a region of uniqueness of a given type associated to a balanced spin–spin resonance of (24). Moreover, such solution can be found by continuation in the space of parameters.

Case of equal bodies $\mathcal{E}_1 = \mathcal{E}_2$ In this case, the Eq. (24) depends on four parameters $(e, \lambda, \hat{q}, \sigma)$, where $\lambda = \lambda_1 = \lambda_2$, $\hat{q} = \hat{q}_1 = \hat{q}_2$ and $\sigma = \sigma_1 = \sigma_2$. From Fig. 10, it looks that a good choice for doing the continuation is in the range $0 \le e \lesssim 0.8$, $0 \le \lambda \lesssim 1$ and $0 \le \hat{q}, \sigma \lesssim 0.01$. In this range, the linear stability of the solution of type $(0, 0)$ associated to the resonance of order $(1 : 1, 1 : 1)$ was investigated in Misquero (2021). Figure 11 shows the stability diagrams of the resonance $(1 : 1, 3 : 2)$ of type $(0, 0)$ and the resonance $(1 : 2, 3 : 2)$ of type $(\frac{\pi}{2}, 0)$ and $(0, 0)$ for different $(\hat{q}, \sigma)$. Let us point out some properties:

(1) Note that a plot with $(\hat{q}, \sigma) = (0, 0)$ is just the superposition of diagrams in Fig. 9, while a plot with $(\hat{q}, \sigma) = (0.01, 0)$ is the superposition of diagrams similar to those in Fig. 10. Then, the effect of the coupling can be seen in the plots with $\sigma \neq 0$.
(2) The effect of the coupling is different in each case: for the resonance $(1 : 2, 3 : 2)$ of type $(0, 0)$, we only see an additional thin unstable region for $e < 0.1$ and $0.25 < \lambda < 1$. For the resonance $(1 : 2, 3 : 2)$ of type $(\frac{\pi}{2}, 0)$, we see that the region with small e becomes unstable, whereas for large e the stability is somewhat altered. Finally, without coupling, the resonance $(1 : 2, 3 : 2)$ of type $(0, 0)$ is unstable for almost all the points, but the coupling introduces the stability for small e. Note that this in agreement with Fig. 6.

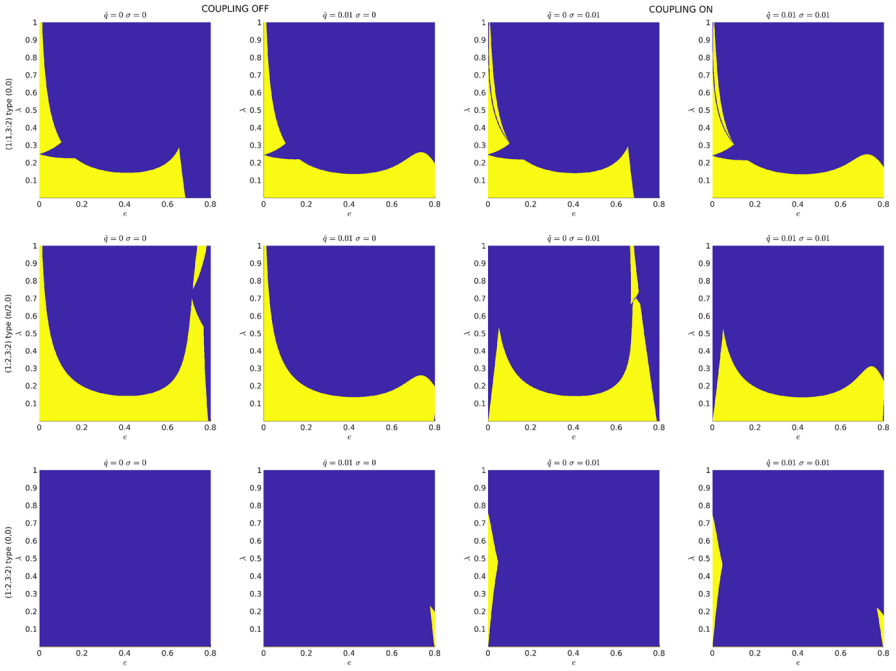

Fig. 11 Regions of (hyperbolic) linear instability of solutions associated to different spin–spin resonances of the problem (24) (case: equal bodies) for different values of the parameters $(\hat{q}, \sigma)$. Blue denotes instability and yellow denotes stability. Each plot has required around 10 min using 15 CPUs and a mesh size 750×750 (Color figure online)

6 Some Numerical Results on the Full and the Keplerian Models

In this section, we provide some results on the comparison between the full and Keplerian problems with particular reference to the conditions under which the decoupling is valid (Sect. 6.1), and we give some numerical results on the interaction between the spin and orbital motions (Sect. 6.2).

6.1 Hamiltonian Approach

It will be useful to write the dynamical equations of the Hamiltonian of the full model (4) in the compact form

$$\dot{z} = J_4 \partial_z H(z), \tag{49}$$

where $z = (r, f, \theta_1, \theta_2, p_r, p_f, p_1, p_2)^{\mathsf{T}}$ and J_4 is defined by (47).

Let us now formulate the Keplerian models (spin–orbit and spin–spin, see Sect. 2.3) as perturbations of the full model, so we can compare both families of models under the condition that the coupling between the spin and the orbit is small. Indeed, we limit to study the stability of the orbital motion, when considering the coupling of the

rotating rigid bodies, and we will just consider the case of equal bodies. Consider a function $\zeta(t)$ that satisfies the equation

$$\dot{\zeta}(t) = J_4 \partial_z H(\zeta(t)) - h(\zeta(t)), \tag{50}$$

where the vector function

$$h(z) = (0, 0, 0, 0, -\partial_r V_{\text{per}}(z), -\partial_f V_{\text{per}}(z), 0, 0)^{\mathsf{T}}$$

is responsible of subtracting the perturbative part of the potential [see Eq. (7)] only in the equations for $\dot{p}_r$ and $\dot{p}_f$. Thus, Eq. (50) represents the Keplerian model including the orbital part: the spin–orbit model corresponds to (50) with $V_{\text{per}} = V_2$ and the spin–spin model with $V_{\text{per}} = V_2 + V_4$. The corresponding equations of motion are (11) and (12), so we can write the solution in the form

$$\zeta(t) = (r(t; a, e),\, f(t; e),\, \theta_1(t),\, \theta_2(t),\, p_r(t; a, e),\, p_f(a, e),\, p_1(t),\, p_2(t)),$$

where a and e are the semimajor axis and the eccentricity of the Keplerian orbit, see (17). Now it is clear that the Keplerian model (50) is not Hamiltonian, even though we can split it into one autonomous Hamiltonian system (orbital part with $V = V_0$) and another non-autonomous one (spin part with $V = V_0 + V_{\text{per}}$). Moreover, unlike for the full model, in a Keplerian model neither the total angular momentum $P_f = p_f + p_1 + p_2$ is conserved,[6] since we can compute that

$$\dot{P}_f(t) = -\sum_{j=1}^{2} \partial_{\theta_j} V_{\text{per}}(r(t; a, e),\, f(t; e), \theta_1(t), \theta_2(t)).$$

We want to investigate the difference between the Keplerian and full models, which, according to (50), are essentially due to the perturbation of the spin on the orbit. Consider the solution $z = z(t) = \zeta(t) - \delta z(t)$ of (49) such that $z(0) = \zeta(0)$. Then, expanding the Eq. (49) up to first order in δz, we obtain that the function $\delta z = \delta z(t)$ satisfies the equation

$$\frac{\mathrm{d}}{\mathrm{d}t}\delta z = J_4 \partial^2_{z,z} H(\zeta(t))\delta z - h(\zeta(t)) \tag{51}$$

with initial condition $\delta z(0) = 0$. In Eq. (51), $\partial^2_{z,z} H(z)$ is the Hessian matrix associated to the Hamiltonian in (4). If the system (51) is stable, then the norm $\|\zeta(t) - z(t)\|$ is bounded. Additionally, it is easy to see that the system (51) is Lyapunov stable if, and only if, the trivial solution of the homogeneous part

$$\dot{y} = J_4 \partial^2_{z,z} H(\zeta(t)) y, \quad y \in \mathbb{R}^8, \tag{52}$$

[6] Instead, the Keplerian assumption results in the conservation of the orbital angular momentum $p_f(t) = \mu r(t; a, e)^2 \dot{f}(t; e) = \mu a^2 \sqrt{1 - e^2}$.

is Lyapunov stable. A general form of $\zeta(t)$ is unknown because, although the orbital part is given by the classical Kepler problem, the spin part is given by a non-autonomous periodic system of nonlinear equations. However, $\zeta(t)$ is a periodic solution at spin–spin resonances, with period 2π for balanced resonances. In such cases, Eq. (52) is an LPH system, some of whose properties were mentioned in Sect. 5.3.

At this point, we wonder if it is possible for the periodic system (52) to be stable. Let us point out an argument supporting a negative answer, even for stable spin–spin resonances. It is known that the periodic solutions of the planar Kepler problem are not linearly stable. This can be easily checked using Poincaré variables (action-angle variables): we obtain a positive eigenvalue for a linear system of constant coefficients. See further related discussions in Boscaggin and Ortega (2016) and Schwarz (1972). We can see that 1 is the only associated Floquet multiplier and has multiplicity four; then, the instability of the periodic solutions of the Kepler problem is not hyperbolic, according to Definition 12, but rather of parabolic kind. From this discussion, we expect that $\zeta(t)$ and $z(t)$ are divergent functions, but we want to know if such divergence is exponential in time, that is, when (52) is hyperbolic unstable.

To this end, suppose that the function $\zeta(t)$ is continuous on a domain of the space of parameters $(a, e; \mathcal{C}_1, \lambda_1, \lambda_2, \sigma_1, \hat{q}_1, \hat{q}_2)$. Note that we add a to the parameters of the spin–spin model because it varies with the orbital initial conditions. On the other hand, the Hamiltonian H depends on the parameters of the full model, we take the independent set $(\mu, \mathcal{C}_1, d_1, d_2, q_1, q_2)$, where the value of μ informs us about the disparity in the masses of the bodies because $\mu = M_1 M_2 = M_1(1 - M_1)$. We can obtain $(\mu, \mathcal{C}_1, d_1, d_2, q_1, q_2)$ from $(a, e; \mathcal{C}_1, \lambda_1, \lambda_2, \sigma_1, \hat{q}_1, \hat{q}_2)$ as follows: First, from (22), we see that, assuming $\sigma_1 > 0$,

$$\mu = \frac{\mathcal{C}_1}{3\sigma_1 a^2}; \tag{53}$$

from this value we can obtain M_1 because $\mu = M_1(1 - M_1)$ with $M_1 \in (0, 1)$. This is enough to write $M_2 = 1 - M_1, \mathcal{C}_2 = 1 - \mathcal{C}_1$ and, from the definitions (22), it holds that

$$d_1 = \frac{\lambda_1 \mathcal{C}_1}{3M_2}, \quad d_2 = \frac{\lambda_2 \mathcal{C}_2}{3M_1}, \quad q_1 = \hat{q}_1 M_1 a^2, \quad q_2 = \hat{q}_2 M_2 a^2.$$

In the following, we take $V_{\text{per}} = V_2 + V_4$. Additionally, the initial conditions associated to $\zeta(t)$ are given by (18), for the orbital part, and the values $\theta_j(0)$, $\dot{\theta}_j(0)$ are such that the spin part satisfies the boundary conditions for the spin–spin problem in a spin–spin resonance of a certain type as in (39). Recall also that, in our units, the Keplerian orbital period is $T = 2\pi$ and $G = a^3$.

As in Sect. 5.3, we can find the region (in the parameters space) of hyperbolic instability and its boundary, that is given by the limit as $\varepsilon \to 0$ of the manifolds that satisfy $\max_{k=1,\ldots,8} |\varphi_k| = 1 + \varepsilon$, where φ_k are the Floquet multipliers of (52). It is important that we focus on a region of the parameters where the corresponding solution associated to a spin–spin resonance is linearly stable.

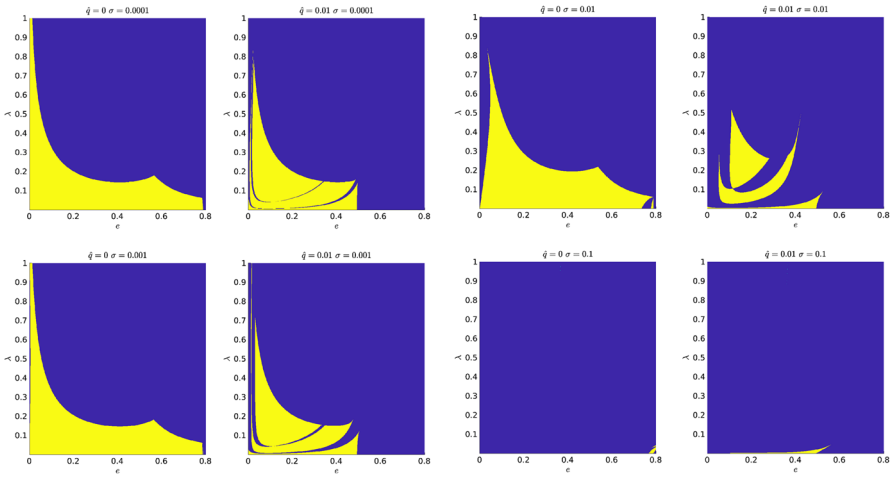

Fig. 12 Regions of (hyperbolic) linear instability of $(1:2,3:2)$ of type $(\pi/2, 0)$ of the Eq. (52) for equal bodies and different values of the parameters. Blue denotes instability and yellow denotes stability. Each plot has required around 10 min using 15 CPUs and a mesh size of 750×750 (Color figure online)

Figure 12 shows the regions of hyperbolic instability of (52) for the particular spin–spin resonance $(1:2,3:2)$ with different values of the parameters. This example provides the following remarks.

(1) We can compare Figs. 12 with 11 for similar values of $\hat{q}$ and σ. In the case of equal bodies ($\mu = 0.25$ and $\mathcal{C}_1 = 0.5$), the value of a is determined by (53): smaller σ also implies further bodies. Although the parameters are not exactly the same in all panels, the plots with $\sigma = 0.0001$ in Fig. 12 can be compared approximately with those with $\sigma = 0$ in Fig. 11.
(2) From the comparison, we see that the plots in Figs. 12 and 11 with $\hat{q} = 0$ are similar for small eccentricities, but, while the unstable regions in Fig. 12 are bigger for larger e. On the other hand, the plots in Fig. 12 with $\hat{q} = 0.01$ include unstable stripes invading the stable regions for small e (they grow with σ), whereas for large e the diagrams become totally unstable.
(3) As we increase σ (closer bodies), the plots become more and more unstable.

We conclude that in this specific example, linear stability occurs in the regions of the parameters with small e.

6.2 Quantitative Numerical Approach

In this section, we want to investigate, from a numerical point of view, the dynamics of the orbital system as perturbed by the rotational motion.

In Sect. 6.1, we analyzed the linear stability of the solution of the Keplerian model $\zeta(t)$ corresponding to a spin–spin resonance. We take a point $(a, e; \mathcal{C}_1, \lambda_1, \lambda_2, \sigma_1, \hat{q}_1, \hat{q}_2)$ and try to quantify the difference between the functions $\zeta(t)$ and $z(t)$.

The orbital motion of $\zeta(t)$ is characterized unambiguously by the set of Keplerian elements (a, e, ω), where $\omega = 0$ is the argument of the periapsis, together with t, the mean anomaly. On the other hand, let the orbital part of the solution $z(t)$ of the full model be given by $(r_F(t),\, f_F(t))$. Then, we can transform the orbital position $\mathbf{r}_F(t) = r_F(t)\exp(if_F(t))$ to the osculating Keplerian elements $(a_F(t), e_F(t), \omega_F(t))$ of the two-body problem using the following expressions. From the geometrical identity $|\dot{\mathbf{r}}_F|^2 = G\left(\frac{2}{r_F} - \frac{1}{a_F}\right)$, we obtain

$$a_F(t) = \left(\frac{2}{r_F} - \frac{\dot{r}_F^2 + \dot{f}_F^2 r_F^2}{G}\right)^{-1}.$$

Now let us define the orbital angular momentum per unit mass $\mathbf{h}_F = \mathbf{r}_F \wedge \dot{\mathbf{r}}_F$, where $\wedge$ is the vector product, and the eccentricity vector

$$\mathbf{e}_F(t) = \frac{\dot{\mathbf{r}}_F \wedge \mathbf{h}_F}{G} - \frac{\mathbf{r}_F}{r_F},$$

whose modulus is given by

$$e_F(t) = \sqrt{1 - \frac{r_F^4 \dot{f}_F^2}{G a_F}}.$$

Whenever $e_F \neq 0$, we can define $\omega_F \in [-\pi, \pi)$ as the polar angle of $\mathbf{e}_F$. The mean anomaly associated to the full model can be defined too, but we will not use it in our study. The balanced spin–spin resonance of order $(m_1 : 2, m_2 : 2)$ in the function $\zeta(t)$ is characterized by the modified resonant angles $\psi_j^{m_j:2}(t) = m_j f(t, e) - 2\theta_j(t)$. Seemingly, the spin part of the solution $z(t)$ of the full model is given by $(\theta_{1,F}(t), \theta_{2,F}(t))$, so, in order to compare with $\zeta(t)$, let us define $\psi_{j,F}^{m_j:2}(t) = m_j f_F(t) - 2\theta_{j,F}(t)$. Now define the functions

$$\delta_a(t) = \frac{a_F(t) - a}{a}, \quad \delta_e(t) = e_F(t) - e, \quad \delta_{\mathrm{res},j}(t) = \psi_j^{m_j:2}(t) - \psi_{j,F}^{m_j:2}(t), \tag{54}$$

where δ_a is the relative deviation in semi-major axis, while δ_e and $\delta_{\mathrm{res},j}$ are the absolute deviations in eccentricity and resonant angles, respectively.

Finally, recall from (1) that we have an expression for a_j in terms of the parameters of the model. Then, for our purpose, we will say that there is a collision if $r_F(t) \leq \mathsf{a}_1 + \mathsf{a}_2$. Now we are in a position to compare the solutions of the full model with respect with those of the Keplerian models.

Then, we plot the evolution of the δ functions in (54) and some Kepler elements of $z(t)$ over 100 revolutions; again, we consider the case of identical bodies and we focus on the resonance $(1 : 1, 3 : 2)$ of type $(0, 0)$. We consider a set of parameters $e = 0$ and $\sigma = 10^{-3}$, so that the bodies are relatively close to each other ($a \approx 39$) and in circular orbits. Beside, we take values of parameters, whose corresponding resonance

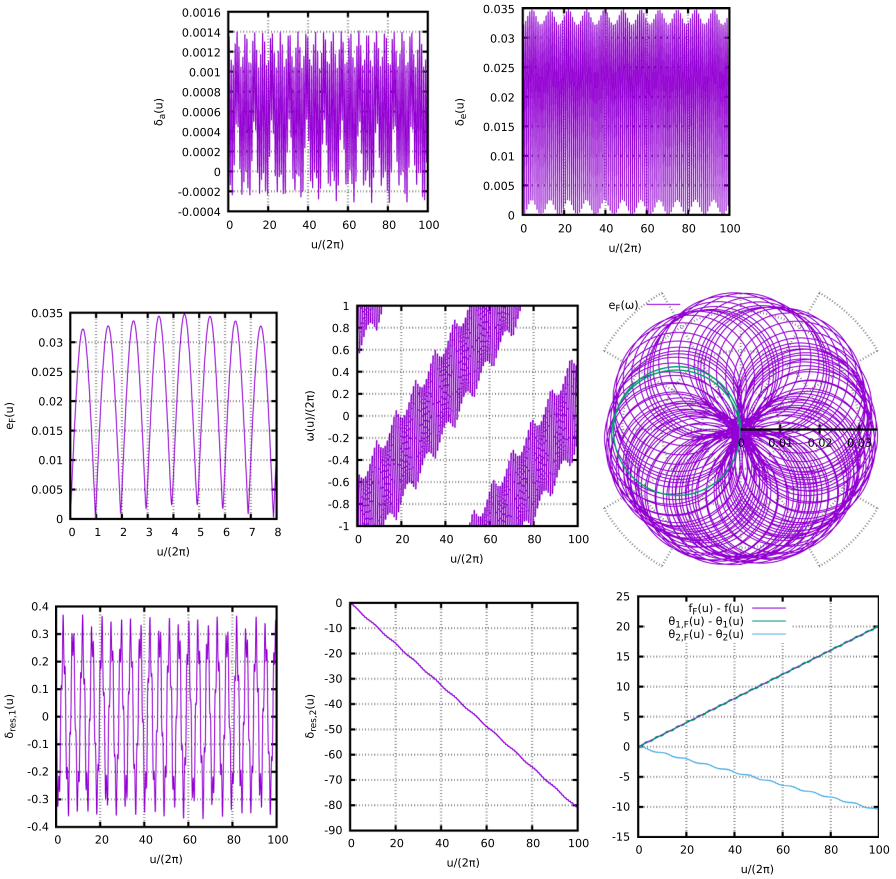

Fig. 13 Evolution of the quantities in (54) and of some Kepler elements in a resonance $(1:1, 3:2)$ of type $(0, 0)$ for different parameter values in the case of equal bodies: $e = 0$, $\lambda = 0.05$, $\hat{q} = 0.01$, $\sigma = 10^{-3}$

is not hyperbolic unstable, say, $\lambda = 0.05$ and $\hat{q} = 0.01$. In addition, Table 2 gives the corresponding Floquet multipliers of both $z(t)$ and $\zeta(t)$.

From Fig. 13, we see that the behavior is regular: the orbit of the full model oscillates regularly very close to the circular orbit of the Keplerian model, with a precession that increases uniformly in average. Actually, in a shorter time scale, the eccentricity vector describes a circles passing through the origin. Also, the variation of the angles is quite regular.

The Floquet multipliers in Table 2 give us additional information. We remark that we display the multipliers of $\zeta(t)$ corresponding to spin and orbit separately, say, the first two rows are the four multipliers of the spin–spin model (24), whereas the third one shows the four coincident multipliers of the Kepler problem. The results confirm that the spin of $\zeta(t)$ is elliptic stable. On the other hand, the multipliers of $z(t)$ are computed with (49). We find out that, although the first case is more regular, the solution is actually hyperbolic unstable. We conclude that, even when there is

Table 2 Modulus and argument of the Floquet multipliers of the functions $z(t)$ and $\zeta(t)$ compared in Fig. 13

	$e = 0, \lambda = 0.05, \hat{q} = 0.01, \sigma = 10^{-3}$	
	Argument	Modulus
$\zeta(t)$	± 1.42	1
	$\pm 7.36 \cdot 10^{-8}$	1
	0	1 (quadruple)
$z(t)$	± 1.41	1
	$\pm 7.64 \cdot 10^{-9}$	1
	$\pm 1.65 \cdot 10^{-1}$	1.09
	$\pm 1.65 \cdot 10^{-1}$	0.915

hyperbolic instability, the solution of full system remains quite close to the solution of the Keplerian system with circular orbit.

7 Conclusions

This research is, primarily, a careful numerical study of the spin–spin model, presented as such in Misquero (2021). For this purpose, we have considered several parallel models describing the planar gravitational dynamics of two ellipsoids under the Assumptions 1 to 3. We distinguish between full and Keplerian models, and also, between spin–orbit and spin–spin models. The known dynamics of the Keplerian spin–orbit problem was used as reference to develop our results.

In first place, we realize that the symmetries of the ellipsoids lead to certain symmetries in the equations of the Keplerian models, and so, to symmetric periodic solutions that structure the overall dynamics. We study the boundary conditions leading to symmetric periodic orbits. We complete this general view by providing conditions for the existence of quasi-periodic solutions. Between the periodic solutions, we focus on a special class that comprises the simplest solutions from the physical interpretation, the balanced spin–orbit and spin–spin resonances. We study the high-dimensional phase space of the spin–spin problem by means of projections of Poincaré maps, taking those of the spin–orbit problem as reference.

First, we see that when one body is spherical, the dynamics of the spin–orbit problem is reproduced with small variations. For two ellipsoids, the projections of the Poincaré maps show structures similar to those of the spin–orbit ones. There is a particular behavior of the spin–spin problem when both bodies are identical, the so-called measure synchronization.

After that, we study existence, multiplicity and linear stability of the solutions in balanced resonances as we vary the parameters of the problem. We focus on the qualitative changes in the stability diagrams produced by the variation of each parameter. We use the case of identical bodies to illustrate our observations most of the time.

In the last part of the paper, we analyze the solutions of the full and the Keplerian models by means of rewriting the equations in a Hamiltonian-like form with the aim to study the stability of the orbital motion under the coupling effect due to the rotation of the rigid bodies. We produce stability diagrams to investigate the linear stability, in a

particular case study. The orbit of the full problem is characterized by Kepler's orbital elements to facilitate the comparison; we compute the deviations in semi-major axis and eccentricity for a grid of values in some parameters.

Although we privileged some particular aspects of the spin–orbit and spin–spin dynamics, we are aware of the fact that many questions are still to be answered or need a deeper investigation. In particular, we concentrated just on specific case studies and, typically, for small parameter values ensuring linear stability. The study of the dynamics for higher values of the parameters needs different mathematical techniques, that may lead to investigate more difficult case studies than those analyzed in the present work, e.g., unequal bodies, highly eccentric orbits, escape orbits, impact configurations. Remarkable results on these topics have been already obtained in the literature (see, e.g., Maciejewski 1995; Scheeres 2002, 2009; Bellerose and Scheeres 2008). Further directions of research might include more theoretical aspects for which the models investigated in the current work could serve as bench tests, for example Arnold diffusion, Nekhoroshev's theorem, the construction of whiskered tori.

Funding Open Access funding provided thanks to the CRUE-CSIC agreement with Springer Nature.

Data Availability The authors declare that the data supporting the findings of this study are available within the article.

Appendix A: Coefficients of the Expansion of the Potential

The full expansion of the potential energy of the Full Two-Body Problem was derived in Boué (2017). Later, Misquero (2021) detailed that expression to the case of planar motion of two ellipsoids, which is given by

$$V = -\frac{GM_1M_2}{r} \sum_{\substack{(l_1,m_1)\in\Upsilon \\ (l_2,m_2)\in\Upsilon}} \Gamma_{l_2,m_2}^{l_1,m_1} \left(\frac{R_1}{r}\right)^{2l_1} \left(\frac{R_2}{r}\right)^{2l_2} \times \mathcal{Z}_{2l_1,2m_1}^{1)} \mathcal{Z}_{2l_2,2m_2}^{2)} \cos(2m_1(\theta_2 - f) + 2m_2(\theta_2 - f)),$$

where

$$\Upsilon = \{(l, m) \in \mathbb{Z}^2 : 0 \le |m| \le l\},$$

and, if we take $L = l_1 + l_2$ and $M = m_1 + m_2$, the constants

$$\Gamma_{l_2,m_2}^{l_1,m_1} = \frac{(-1)^{L-M}}{4^L\sqrt{(2l_1-2m_1)!(2l_1+2m_1)!(2l_2-2m_2)!(2l_2+2m_2)!}} \times \frac{(2L-2M)!(2L+2M)!}{(L-M)!(L+M)!}$$

are numbers dealing with the interaction between the extended bodies. On the other hand, R_j and $\mathcal{Z}_{2l_j,2m_j}^{j)}$ are, respectively, the mean radius and the Stokes coefficients of each $\mathcal{E}_j$. The quantities $\mathcal{Z}_{l,m}^{j)}$ provide the expansion of the potential created for the body $\mathcal{E}_j$. They are related to the usual parameters $C_{l,m}^{j)}$ and $S_{l,m}^{j)}$ by

$$C_{l,m}^{j)} + iS_{l,m}^{j)} = (-1)^m \frac{2}{1+\delta_{m,0}}\sqrt{\frac{(l-m)!}{(l+m)!}}\bar{\mathcal{Z}}_{l,m}^{j)}, \quad m \geq 0,$$

where $\delta_{m,n}$ is the Kronecker delta.

Appendix B: A Different Formulation of the Equations of Motion

To perform the integration of (12), it is convenient to adopt the eccentric anomaly u as independent variable, according to the following procedure.

Let us write the Eq. (12) as

$$C_j \frac{d^2\theta_j}{dt^2}(t) + \left(\frac{a}{r}\right)^5 \varepsilon_j F_j(t,\theta) = 0, \quad j = 1,2, \tag{55}$$

where $\theta = (\theta_1, \theta_2)$, $C_1 + C_2 = 1$ and $F_j = \partial_{\theta_j}(V_2 + V_4)$, $j = 1, 2$. The explicit expression for F_1 and F_2 is given by

$$\begin{aligned} F_1(t,\theta) &= \left(\left(\frac{r}{a}\right)^2 + \frac{5}{4}\left(\hat{q}_2 + \frac{5}{7}\hat{q}_1\right)\right)\sin(2\theta_1 - 2f) \\ &\quad + \frac{25\hat{d}_1}{8}\sin(4\theta_1 - 4f) + \frac{3\hat{d}_2}{8}\sin(2\theta_1 - 2\theta_2) \\ &\quad + \frac{35\hat{d}_2}{8}\sin(2\theta_2 + 2\theta_1 - 4f) \\ F_2(t,\theta) &= \left(\left(\frac{r}{a}\right)^2 + \frac{5}{4}\left(\hat{q}_1 + \frac{5}{7}\hat{q}_2\right)\right)\sin(2\theta_2 - 2f) + \frac{25\hat{d}_2}{8}\sin(4\theta_2 - 4f) \\ &\quad - \frac{3\hat{d}_1}{8}\sin(2\theta_1 - 2\theta_2) + \frac{35\hat{d}_1}{8}\sin(2\theta_2 + 2\theta_1 - 4f). \end{aligned} \tag{56}$$

Let us consider the change of variables given by the Kepler's equation

$$x_j(u) = \theta_j(u - e\sin u), \quad j = 1,2.$$

Then, we have

$$\frac{d^2\theta_j}{dt^2}(t) = \left(\frac{a}{r(u)}\right)^2 \frac{d^2x_j}{du^2}(u) - \left(\frac{a}{r(u)}\right)^3 \frac{dx_j}{du}(u)e\sin u, \quad j = 1, 2,$$

so that, assuming $C_j \neq 0$, (55) becomes

$$\frac{d^2x_j}{du^2}(u) - \frac{a}{r(u)}\frac{dx_j}{du}(u)e\sin u + \left(\frac{a}{r(u)}\right)^3 \frac{\varepsilon_j}{C_j}F_j(u, x) = 0, \quad j = 1, 2. \tag{57}$$

We can write the system (57) as

$$\begin{aligned}
\frac{dx_j}{du}(u) &= y_j(u)\\
\frac{dy_j}{du}(u) &= \frac{a}{r(u)}y_j(u)e\sin u - \left(\frac{a}{r(u)}\right)^3 \frac{\varepsilon_j}{C_j}F_j(u, x),
\end{aligned}$$

for $j = 1, 2$ and $x = (x_1, x_2)$. From the well-known relations used in the study of Kepler's problem

$$\cos f = \frac{\cos u - e}{1 - e\cos u}, \quad \sin f = \frac{\sqrt{1-e^2}\sin u}{1 - e\cos u},$$

we can define the functions $s = s(x_j)$, $c = c(x_j)$ as

$$\begin{aligned}
s(x_j) &= \sin(2x_j)(2\cos^2 f - 1) - \cos(2x_j)2\cos f \sin f\\
c(x_j) &= \cos(2x_j)(2\cos^2 f - 1) + \sin(2x_j)2\cos f \sin f,
\end{aligned}$$

so that F_1 and F_2 in (56) take the form

$$\begin{aligned}
F_1(u, x) &= \left(\left(\frac{r(u)}{a}\right)^2 + \frac{5}{4}\left(\hat{q}_2 + \frac{5}{7}\hat{q}_1\right)\right)s(x_1)\\
&\quad + \frac{25\hat{d}_1}{4}s(x_1)c(x_1) + \frac{3\hat{d}_2}{8}\sin(2x_1 - 2x_2) + \frac{35\hat{d}_2}{4}s(x_1 + x_2)c(x_1 + x_2)\\
F_2(u, x) &= \left(\left(\frac{r(u)}{a}\right)^2 + \frac{5}{4}\left(\hat{q}_1 + \frac{5}{7}\hat{q}_2\right)\right)s(x_2) + \frac{25\hat{d}_2}{4}s(x_1)c(x_1)\\
&\quad - \frac{3\hat{d}_1}{8}\sin(2x_1 - 2x_2) + \frac{35\hat{d}_1}{4}s(x_1 + x_2)c(x_1 + x_2).
\end{aligned}$$

Appendix C: Expansion of V_2 and V_4

We give below the expansion of V_2 and V_4 up to second order in the eccentricity:

$$
\begin{aligned}
V_2 = &-\frac{3d_1e^2GM_2\cos(2\theta_1)}{8a^3} - \frac{3d_2e^2GM_1\cos(2\theta_2)}{8a^3} - \frac{27d_1e^2GM_2\cos(2t-2\theta_1)}{8a^3}\\
&- \frac{3d_1e^2GM_2\cos(4t-2\theta_1)}{4a^3} - \frac{27d_2e^2GM_1\cos(2t-2\theta_2)}{8a^3}\\
&- \frac{3d_2e^2GM_1\cos(4t-2\theta_2)}{4a^3}\\
&- \frac{9d_1eGM_2\cos(t-2\theta_1)}{8a^3} - \frac{9d_1eGM_2\cos(3t-2\theta_1)}{8a^3} - \frac{9d_2eGM_1\cos(t-2\theta_2)}{8a^3}\\
&- \frac{9d_2eGM_1\cos(3t-2\theta_2)}{8a^3} - \frac{3d_1GM_2\cos(2t-2\theta_1)}{4a^3} - \frac{3d_2GM_1\cos(2t-2\theta_2)}{4a^3}\\
&- \frac{3e^2GM_2q_1\cos(2t)}{8a^3} - \frac{3e^2GM_1q_2\cos(2t)}{8a^3} - \frac{9e^2GM_2q_1}{8a^3} - \frac{9e^2GM_1q_2}{8a^3}\\
&- \frac{3eGM_2q_1\cos(t)}{4a^3}\\
&- \frac{3eGM_1q_2\cos(t)}{4a^3} - \frac{GM_2q_1}{4a^3} - \frac{GM_1q_2}{4a^3},\\
V_4 = &-\frac{225GM_2q_1^2e^2}{112a^5M_1} - \frac{225G\cos(2t)M_2q_1^2e^2}{224a^5M_1} - \frac{225GM_1q_2^2e^2}{112a^5M_2}\\
&- \frac{225G\cos(2t)M_1q_2^2e^2}{224a^5M_2}\\
&- \frac{105G\cos(2t-2\theta_1-2\theta_2)d_1d_2e^2}{16a^5} - \frac{525G\cos(4t-2\theta_1-2\theta_2)d_1d_2e^2}{16a^5}\\
&- \frac{315G\cos(6t-2\theta_1-2\theta_2)d_1d_2e^2}{32a^5} - \frac{45G\cos(2\theta_1-2\theta_2)d_1d_2e^2}{16a^5}\\
&- \frac{45G\cos(2t+2\theta_1-2\theta_2)d_1d_2e^2}{64a^5} - \frac{45G\cos(2t-2\theta_1+2\theta_2)d_1d_2e^2}{64a^5}\\
&- \frac{225Gd_1^2M_2e^2}{224a^5M_1}\\
&- \frac{225G\cos(2t)d_1^2M_2e^2}{448a^5M_1} - \frac{75G\cos(2t-4\theta_1)d_1^2M_2e^2}{32a^5M_1}\\
&- \frac{375G\cos(4t-4\theta_1)d_1^2M_2e^2}{32a^5M_1}\\
&- \frac{225G\cos(6t-4\theta_1)d_1^2M_2e^2}{64a^5M_1} - \frac{75G\cos(2t-2\theta_2)d_2q_1e^2}{8a^5}\\
&- \frac{165G\cos(4t-2\theta_2)d_2q_1e^2}{64a^5}\\
&- \frac{135G\cos(2\theta_2)d_2q_1e^2}{64a^5} - \frac{375G\cos(2t-2\theta_1)d_1M_2q_1e^2}{56a^5M_1}
\end{aligned}
$$

$$
\begin{aligned}
&- \frac{825G\cos(4t-2\theta_1)d_1M_2q_1e^2}{448a^5M_1} \\
&- \frac{675G\cos(2\theta_1)d_1M_2q_1e^2}{448a^5M_1} - \frac{75G\cos(2t-2\theta_1)d_1q_2e^2}{8a^5} \\
&- \frac{165G\cos(4t-2\theta_1)d_1q_2e^2}{64a^5} \\
&- \frac{135G\cos(2\theta_1)d_1q_2e^2}{64a^5} - \frac{45Gq_1q_2e^2}{8a^5} - \frac{45G\cos(2t)q_1q_2e^2}{16a^5} \\
&- \frac{375G\cos(2t-2\theta_2)d_2M_1q_2e^2}{56a^5M_2} \\
&- \frac{825G\cos(4t-2\theta_2)d_2M_1q_2e^2}{448a^5M_2} - \frac{675G\cos(2\theta_2)d_2M_1q_2e^2}{448a^5M_2} - \frac{225Gd_2^2M_1e^2}{224a^5M_2} \\
&- \frac{225G\cos(2t)d_2^2M_1e^2}{448a^5M_2} \\
&- \frac{75G\cos(2t-4\theta_2)d_2^2M_1e^2}{32a^5M_2} - \frac{375G\cos(4t-4\theta_2)d_2^2M_1e^2}{32a^5M_2} \\
&- \frac{225G\cos(6t-4\theta_2)d_2^2M_1e^2}{64a^5M_2} \\
&- \frac{225G\cos(t)M_2q_1^2e}{224a^5M_1} - \frac{225G\cos(t)M_1q_2^2e}{224a^5M_2} - \frac{525G\cos(3t-2\theta_1-2\theta_2)d_1d_2e}{64a^5} \\
&- \frac{525G\cos(5t-2\theta_1-2\theta_2)d_1d_2e}{64a^5} - \frac{45G\cos(t+2\theta_1-2\theta_2)d_1d_2e}{64a^5} \\
&- \frac{45G\cos(t-2\theta_1+2\theta_2)d_1d_2e}{64a^5} - \frac{225G\cos(t)d_1^2M_2e}{448a^5M_1} \\
&- \frac{375G\cos(3t-4\theta_1)d_1^2M_2e}{128a^5M_1} \\
&- \frac{375G\cos(5t-4\theta_1)d_1^2M_2e}{128a^5M_1} - \frac{75G\cos(t-2\theta_2)d_2q_1e}{32a^5} \\
&- \frac{75G\cos(3t-2\theta_2)d_2q_1e}{32a^5} \\
&- \frac{375G\cos(t-2\theta_1)d_1M_2q_1e}{224a^5M_1} - \frac{375G\cos(3t-2\theta_1)d_1M_2q_1e}{224a^5M_1} \\
&- \frac{75G\cos(t-2\theta_1)d_1q_2e}{32a^5} \\
&- \frac{75G\cos(3t-2\theta_1)d_1q_2e}{32a^5} - \frac{45G\cos(t)q_1q_2e}{16a^5} - \frac{375G\cos(t-2\theta_2)d_2M_1q_2e}{224a^5M_2} \\
&- \frac{375G\cos(3t-2\theta_2)d_2M_1q_2e}{224a^5M_2} - \frac{225G\cos(t)d_2^2M_1e}{448a^5M_2} \\
&- \frac{375G\cos(3t-4\theta_2)d_2^2M_1e}{128a^5M_2}
\end{aligned}
$$

$$
\begin{aligned}
&- \frac{375G\cos(5t-4\theta_2)d_2^2M_1e}{128a^5M_2} - \frac{45GM_2q_1^2}{224a^5M_1} - \frac{45GM_1q_2^2}{224a^5M_2} \\
&- \frac{105G\cos(4t-2\theta_1-2\theta_2)d_1d_2}{32a^5} \\
&- \frac{9G\cos(2\theta_1-2\theta_2)d_1d_2}{32a^5} - \frac{45Gd_1^2M_2}{448a^5M_1} - \frac{75G\cos(4t-4\theta_1)d_1^2M_2}{64a^5M_1} \\
&- \frac{15G\cos(2t-2\theta_2)d_2q_1}{16a^5} - \frac{75G\cos(2t-2\theta_1)d_1M_2q_1}{112a^5M_1} \\
&- \frac{15G\cos(2t-2\theta_1)d_1q_2}{16a^5} - \frac{9Gq_1q_2}{16a^5} - \frac{75G\cos(2t-2\theta_2)d_2M_1q_2}{112a^5M_2} \\
&- \frac{45Gd_2^2M_1}{448a^5M_2} - \frac{75G\cos(4t-4\theta_2)d_2^2M_1}{64a^5M_2}.
\end{aligned}
$$

References

Arnol'd, V.I.: Proof of a theorem of A.N. Kolmogorov on the invariance of quasi-periodic motions under small perturbations. Russ. Math. Surv. **18**, 9–36 (1963)

Batygin, K., Morbidelli, A.: Spin–spin coupling in the solar system. Astrophys. J. **810**, 110 (2015). https://doi.org/10.1088/0004-637x/810/2/110

Beletskii, V.V.: Motion of an artificial satellite about its center of mass, Mechanics of Space Flight, Israel Program for Scientific Translations; [available from the U.S. Dept. of Commerce, Clearinghouse for Federal Scientific and Technical Information, Springfield, Va.]. Jerusalem (1966). https://archive.org/details/nasa_techdoc_19670006100

Beletskii, V.V., Lavrovskii, E.K.: On the theory of the resonance rotation of Mercury. Astronomicheskii Zhurnal **52**, 1299–1308 (1975). https://ui.adsabs.harvard.edu/abs/1975AZh....52.1299B

Bellerose, J., Scheeres, D.J.: Energy and stability in the Full Two Body Problem. Celest. Mech. Dyn. Astron. **100**, 63–91 (2008). https://doi.org/10.1007/s10569-007-9108-3

Boscaggin, A., Ortega, R.: Periodic solutions of a perturbed Kepler problem in the plane: from existence to stability. J. Differ. Equ. **261**, 2528–2551 (2016). https://doi.org/10.1016/j.jde.2016.05.004

Boué, G.: The two rigid body interaction using angular momentum theory formulae. Celest. Mech. Dyn. Astron. **128**, 261–273 (2017). https://doi.org/10.1007/s10569-017-9751-2

Boué, G., Laskar, J.: Spin axis evolution of two interacting bodies. Icarus **201**, 750–767 (2009). https://doi.org/10.1016/j.icarus.2009.02.001

Calleja, R., Celletti, A., Gimeno, J., de la Llave, R.: Efficient and accurate KAM tori construction for the dissipative spin–orbit problem using a map reduction. J. Nonlinear Sci. **32**, 1–40 (2022). https://doi.org/10.1007/s00332-021-09767-5

Calleja, R., Celletti, A., Gimeno, J., de la Llave, R.: KAM quasi-periodic tori for the dissipative spin–orbit problem. Commun. Nonlinear Sci. Numer. Simul. **106**, 106099 (2022). https://doi.org/10.1016/j.cnsns.2021.106099

Calleja, R.C., Celletti, A., Gimeno, J., de la Llave, R.: Accurate computations up to break-down of quasi-periodic attractors in the dissipative spin–orbit problem. Preprint (2022)

Celletti, A.: Analysis of resonances in the spin–orbit problem in celestial mechanics: the synchronous resonance. I. Z. Angew. Math. Phys. **41**, 174–204 (1990). https://doi.org/10.1007/BF00945107

Celletti, A.: Stability and Chaos in Celestial Mechanics, vol. 01. Springer, Berlin (2010). https://doi.org/10.1007/978-3-540-85146-2

Celletti, A., Chierchia, L.: Hamiltonian stability of spin–orbit resonances in celestial mechanics. Celest. Mech. Dyn. Astron. **76**, 229–240 (2000). https://doi.org/10.1023/A:1008341317257

Celletti, A., Chierchia, L.: Measures of basins of attraction in spin–orbit dynamics. Celest. Mech. Dyn. Astron. **101**, 159–170 (2008). https://doi.org/10.1007/s10569-008-9142-9

Celletti, A., Chierchia, L.: Quasi-periodic attractors in celestial mechanics. Arch. Ration. Mech. Anal. **191**, 311–345 (2009). https://doi.org/10.1007/s00205-008-0141-5

Celletti, A., Falcolini, C., Locatelli, U.: On the break-down threshold of invariant tori in four dimensional maps. Regul. Chaotic Dyn. **9**, 227–253 (2004). https://doi.org/10.1070/RD2004v009n03ABEH000278

Colombo, G., Shapiro, I.I.: The rotation of the planet Mercury. Astrophys. J. **145**, 296 (1966). https://doi.org/10.1086/148762

De Vogelaere, R.: On the structure of symmetric periodic solutions of conservative systems, with applications. In: Contributions to the Theory of Nonlinear Oscillations, Annals of Mathematics Studies, vol. IV, no. 41, pp. 53–84. Princeton University Press, Princeton (1958)

Ekeland, I.: Convexity Methods in Hamiltonian Mechanics. Ergebnisse der Mathematik und ihrer Grenzgebiete: A Series of Modern Surveys in Mathematics. Folge 3, vol. 19. Springer, Berlin (1990). https://doi.org/10.1007/978-3-642-74331-3

Goldreich, P., Peale, S.: Spin orbit coupling in the solar system. Astron. J. **71**, 425 (1966). https://doi.org/10.1086/109947

Goldstein, H.: Classical Mechanics. Addison-Wesley, Reading (1980)

Greene, J.M.: A method for determining a stochastic transition. J. Math. Phys. **20**, 1183–1201 (1979). https://doi.org/10.1063/1.524170

Hampton, A., Zanette, D.H.: Measure synchronization in coupled Hamiltonian systems. Phys. Rev. Lett. **83**, 2179–2182 (1999). https://doi.org/10.1103/PhysRevLett.83.2179

Hou, X., Xin, X.: A note on the spin–orbit, spin–spin, and spin–orbit–spin resonances in the binary minor planet system. Astron. J. **154**, 257 (2017). https://doi.org/10.3847/1538-3881/aa96ab

Jorba, À., Zou, M.: A software package for the numerical integration of ODEs by means of high-order Taylor methods. Exp. Math. **14**, 99–117 (2005). http://projecteuclid.org/euclid.em/1120145574

Kinoshita, H.: First-order perturbations of the two finite body problem. Publ. Astron. Soc. Jpn. **24**, 423 (1972)

Kolmogorov, A.N.: On the conservation of conditionally periodic motions under small perturbation of the Hamiltonian. Dokl. Akad. Nauk. SSR **98**, 2–3 (1954)

Krein, M.: Generalization of certain investigations of A.M. Lyapunov on linear differential equations with periodic coefficients. Dokl. Akad. Nauk USSR **73**, 445–448 (1950)

Lamb, J.S.W., Roberts, J.A.G.: Time-reversal symmetry in dynamical systems: a survey. **112**, 1–39 (1998). https://doi.org/10.1016/S0167-2789(97)00199-1. Time-reversal symmetry in dynamical systems (Coventry, 1996)

Laskar, J., Robutel, P.: The chaotic obliquity of the planets. Nature **361**, 608–612 (1993). https://doi.org/10.1038/361608a0

Maciejewski, A.J.: Reduction, relative equilibria and potential in the two rigid bodies problem. Celest. Mech. Dyn. Astron. **63**, 1–28 (1995). https://doi.org/10.1007/BF00691912

Magnus, W., Winkler, S.: Hill's Equation. Dover, New York (1979)

Misquero, M.: The spin–spin model and the capture into the double synchronous resonance. Nonlinearity **34**, 2191–2219 (2021). https://doi.org/10.1088/1361-6544/abc4d8

Misquero, M., Ortega, R.: Some rigorous results on the 1:1 resonance of the spin–orbit problem. SIAM J. Appl. Dyn. Syst. **19**, 2233–2267 (2020). https://doi.org/10.1137/19M1294241

Moser, J.: On invariant curves of area-preserving mappings of an annulus. Nachr. Akad. Wiss. Göttingen Math.-Phys. Kl. II **1962**, 1–20 (1962)

Nadoushan, M.J., Assadian, N.: Chirikov diffusion in the sphere-ellipsoid binary asteroids. Nonlinear Dyn. (2016). https://doi.org/10.1007/s11071-016-2799-9

Nadoushan, M.J., Assadian, N.: Geography of the rotational resonances and their stability in the ellipsoidal full two body problem. Icarus **265**, 175–186 (2016). https://doi.org/10.1016/j.icarus.2015.10.011

Scheeres, D.J.: Stability in the full two-body problem. Celest. Mech. Dyn. Astron. **83**, 155–169 (2002). https://doi.org/10.1023/A:1020143116091

Scheeres, D.J.: Stability of the planar full 2-body problem. Celest. Mech. Dyn. Astron. **104**, 103–128 (2009). https://doi.org/10.1007/s10569-009-9184-7

Schwarz, H.R.: Stability of Kepler motion. Comput. Methods Appl. Mech. Eng. **1**, 279–299 (1972). https://doi.org/10.1016/0045-7825(72)90009-6

Verner, J.: Explicit Runge–Kutta methods with estimates of the local truncation error. SIAM J. Numer. Anal. **15**, 772–790 (1978)

Wisdom, J., Peale, S.J., Mignard, F.: The chaotic rotation of Hyperion. Icarus **58**, 137–152 (1984). https://doi.org/10.1016/0019-1035(84)90032-0

Yakubovich, V.A., Starzhinskii, V.M.: Linear Differential Equations with Periodic Coefficients. Wiley, New York (1975)

Zlatoustov, V., Ohotzimsky, D., Sarychev, V., Torzhevsky, A.: Investigation of a satellite oscillations in the plane of an elliptic orbit. In: Görtler, H. (ed.) Applied Mechanics. Proceedings of the Eleventh International Congress of Applied Mechanics Munich (Germany) 1964, pp. 436–439. Springer, Berlin (1966). https://doi.org/10.1007/978-3-662-29364-5_59